UNIVERSITY OF SASSARI

International PhD School in Biomolecular and Biotechnological Sciences

Curriculum Biochemistry, Physiology and Molecular Biology

Cycle XXVIII

Director: Professor Leonardo A. Sechi

Impact of the diabetic environment on the fetal vasculature: role of microRNA-101 and Enhancer of Zeste Homologue 2

Supervisor:

Prof. Gianfranco Pintus

PhD Candidate:

Dr. Mariantonella Vardeu

Co-Supervisor:

Prof. Costanza Emanueli

ACADEMIC YEAR 2014-2015

La presente tesi è stata prodotta nell'ambito della scuola di dottorato in Scienze Biomolecolari e Biotecnologiche dell'Università degli Studi di Sassari, a.a. 2014/2015 – XXVIII ciclo, con il supporto di una borsa di studio finanziata con le risorse del P.O.R. SARDEGNA F.S.E. 2007-2013 - Obiettivo competitività regionale e occupazione, Asse IV Capitale umano, Linea di Attività l.3.1.

Table of contents

Thesis Summary 6

Acronyms and Abbreviations 8

Chapter I – Introduction 11

1.1 Gestational diabetes mellitus (GDM) 12

1.1.1 Definition and pathophysiology 12

1.1.2 GDM and long-term maternal outcomes 13

1.1.3 Fetal programming and GDM long-term outcomes for the offspring 14

1.1.4 Diagnosis and screening 15

1.1.5 Treatment of GDM 17

1.2 Maternal hyperglycemia and fetal endothelial dysfunction 19

1.2.1 Biochemical and cellular signaling underlying diabetic vascular complications 19

1.2.2 "Metabolic memory" and GDM vascular complications 21

1.2.3 Models of metabolic memory 22

1.3 Role of epigenetic factors in GDM vascular complications 24

1.3.1 Epigenetics and transcriptional regulation of gene expression 24

1.3.2 Transmission of epigenetic modifications 26

1.3.3 Role for microRNAs in epigenetic regulation 27

1.3.4 MiRNAs as novel regulators of endothelial function 29

1.3.5 Enhancer of Zeste Homologue 2 and its role in angiogenesis 30

1.3.6 Enhancer of Zeste Homologue 2 and its novel isoform: EZH2-β 31

1.4 Diagnostic and therapeutic potential of miRNAs in GDM vascular complications 34

1.4.1 MiRNAs with diagnostic potential for vascular complications 34

1.4.2 MiRNAs as therapeutic targets for angiogenesis 35

Chapter II - Aim of the Study 37

Aim of the study 38

Chapter III – Materials and Methods 39

3.1 Study subjects and ethics 40
3.2 Isolation and culture of Human Umbilical Vein Endothelial cells (HUVECs) 40
3.3 Immunocytochemistry 41
3.4 Experiments concerning the exposure of cells to high glucose 42
3.5 MiRNA and siRNA transient HUVECs transfection 42
3.6 HUVECs adenoviral transduction experiments 43
3.7 Apoptosis assay 43
3.8 BrdU proliferation assay 44
3.9 *In vitro* scratch assay 45
3.10 Tube formation assay on Matrigel 45
3.11 Total RNA isolation for mRNA and miRNA analysis 46
3.12 Quantitative Reverse Transcription Polymerase Chain Reaction (qRT-PCR) for mRNA 46
3.13 Quantitative Reverse Transcription Polymerase Chain Reaction (qRT-PCR) for microRNA 47
3.14 Western blot experiments 47
3.15 Chromatin immunoprecipitation (ChIP) 48
3.16 Molecular cloning of mir-101 promoter and activity assessment by luciferase reporter assay 49
3.17 Statistical analysis 50
Chapter IV - Results 51
4.1 HUVECs isolation and characterization 52
4.2 Gestational diabetes mellitus induces phenotypic alterations in HUVECs .. 53
4.3 MiR-101 is upregulated in HUVECs exposed to diabetic uterine environment 55
4.4 Effect of miR-101 dysregulation on GDM-HUVEC phenotype 56
4.5 Enhancer of Zeste Homologue 2 is downregulated in GDM-HUVECs 59
4.6 MiR-101 downregulates EZH2 expression in GDM-HUVECs 62

4.7 GDM reduces EZH2 and H3K27m3 occupancy at the miR-101 locus transcriptional regulatory region 64

4.8 EZH2β inhibits miR-101 transcription in HUVECs 65

4.9 *In vitro* exposure of healthy HUVECs to high concentrations of glucose lowers EZH2 binding to the miR-101 promoter and increases miR-101 expression 66

4.10 Effect of EZH2 overexpression on phenotypic alterations in GDM-HUVECs 67

Chapter V – Discussion and Conclusions 69

Chapter VI – References 73

Acknowledgments 85

Thesis Summary

Gestational diabetes mellitus (GDM) is a specific form of diabetes affecting about 7% of all pregnancies [1]. GDM usually reverses after delivery, but altered glucose homeostasis harms the mother. Moreover, since it translates into fetal hyperglycemia, GDM can affect the healthy development of the fetus, with consequences that can be experienced *in utero* and/or at different stages of post-natal life. In particular, the child from a GDM pregnancy has higher chance of developing type 2 diabetes (T2D) and cardiovascular diseases (CVD) [2–4]. Several clinical trials and epidemiological studies in patients with either type 1 or 2 diabetes show that exposure to prolonged hyperglycemia leaves a long-lasting impression on vascular cells leading to the development of vascular complications which persist after glycemic control is achieved. The same studies also suggested that a good glycemic control can delay the onset of vascular complications in diabetic subjects [5].

The term “epigenetic” refers to heritable changes in the cellular phenotype that do not involve changes in the genotype. There are different kind of epigenetic modifications including methylation and acetylation of histones, and DNA methylation, and these modifications influence gene expression [6,7]. Although the precise mechanistic insight is still unclear, epigenetic regulation might be involved in the long-lasting effect of diabetes on the vascular system [8].

In this study, we focused our attention on the methyltransferase Enhancer of Zeste Homologue 2 (EZH2), that is part of the Polycomb Repressor Complex 2 (PRC2) and plays an essential role in the epigenetic maintenance of the trimethylation of lysine 27 on histone3 (H3K27me3). It has been recently shown that alternative splicing of the EZH2 locus yields two major transcriptional variants: EZH2α and EZH2β [9].The two isoforms can each not only regulate distinct targets, but also share gene expression networks, making the regulation of transcription based on the deposition of the H3K27 histone mark more complex than previously anticipated [9].

MicroRNAs (miRNAs) are single-stranded, non-coding RNAs of 19-25 nucleotides that normally bind the 3’-untranslated region of target mRNAs and contribute to the post-transcriptional regulation of gene expression. A link has been shown between EZH2 and some miRNAs [10,11]. In particular, miR-101 reportedly affects endothelial

function and angiogenesis by targeting and inhibiting EZH2 under normoglycemic conditions [12].

The aim of our study was to investigate the impact of GDM on fetal endothelial biology. To this end, we isolated human umbilical vein endothelial cells (HUVECs) from the umbilical cords of GDM and control healthy pregnancies. These cells represent a good cell model allowing for non-invasive analyses of the effect of the uterine environment on the fetal endothelium. The first objective was to investigate the impact of GDM on the functional capacity of HUVECs, with particular focus on apoptosis, migration, proliferation and tube formation. Next, we evaluated the expression of EZH2 (both α and β isoforms) and miR-101 to see whether they affect endothelial function in diabetic conditions. We first found that cultured GDM-HUVECs demonstrated decreased survival and functional capabilities in comparison with HUVECs obtained from healthy non-diabetic mothers. Additionally, we have identified a novel underlying mechanism involving miR-101 and EZH2 in GDM-elicited endothelial dysfunction. In particular, we have found that in HUVECs, EZH2 is both a target of, and a transcriptional repressor for, miR-101. Notably we found that among the two recently identified EZH2 isoforms, EZH2β is the only one which is both a target of GDM and a mediator of some of the GDM-related damaging effects on HUVECs.

Acronyms and Abbreviations

ACOG	American Congress of Obstetricians and Gynecologist
Ad	Adenovirus
ADA	American Diabetes Association
AGE	Advanced glycation end product
BrDU	5-bromo-2'deoxy-uridine
CD-144	Cluster of differentiation 144
CD-31	Cluster of differentiation 31
ChIP	Chromatin immunoprecipitation
CVD	Cardiovascular disease
DCCT	Diabetes Control and Complications Trial
DGCR8	Di George syndrome critical region
DM	Diabetes mellitus
DMEs	DNA demethylase
DNMTs	DNA methyltransferases
ECM	Extra cellular matrix
ECs	Endothelial cells
EDIC	Epidemiology of Diabetic Complications and Interventions Trial
EDTA	Ethylenediaminetetraacetic acid
EED	Embryonic ectoderm development
EGTA	Ethylene glycol tetraacetic acid
eNOS	Endothelial nitric oxide synthase
ES	Endocrine Society
EZH2	Enhancer of zeste homologue 2
FCS	Fetal calf serum
FFAs	Free fatty acids
GAPDH	Glyceraldehyde-3-phosphate dehydrogenase
GDM	Gestational diabetes mellitus
H3K27me3	Trimethylation of lysine 27 on histone H3
HATs	Histone acetyltransferases
HDACs	Histone deacetylases
HG	High D-glucose

HMTs	Histone methyltransferases
HPL	Human placental lactogen
HRP	Horse radish peroxidase
HUVECs	Human umbilical vein endothelial cells
IADPSG	International Association of Diabetes and Pregnancy Study Groups
JHDM2A	JmjC domain containing histone demethylase 2A
KDMs	Histone demethylases
LSD1	Lysine demethylase 1
MAPK	Mitogen-activated protein kinase
MBPs	Methylated DNA-binding proteins
MCP-1	Monocyte chemoattractant protein-1
miRNA	microRNA
MOI	Multiplicity of infection
NBCS	Newborn calf serum
NF-kB	Nuclear factor kappa B
NG	Normal D-glucose
NO	Nitric oxide
NR	Nuclear receptor
OGGT	Oral glucose tolerance test
PARP	Poly-ADP-ribose polymerase
PBS	Phosphate-buffered saline
PcG	Polycomb-Group
PFA	Paraformaldehyde
PKC	Protein kinase C
PRC1	Polycomb repressor complex 1
PRC2	Polycomb repressor complex 2
Pre-miRNA	Precursor miRNA
Pri-miRNA	Primary miRNA
qPCR	Quantitative polymerase chain reaction
SD	Standard deviation
SDS	Sodium dodecyl sulfate
SEM	Standard error of the mean
STZ	Streptozotocin
SUZ12	Suppressor of zeste 12

T1D	Type 1 diabetes
T2D	Type 2 diabetes
TNF-α	Tumor necrosis factor-α
TRBP	Transactivation response RNA binding protein
UKPDS	United Kingdom Prospective Diabetes Study
VCAM-1	Vascular cell adhesion molecule-1
vWF	Von Willebrand Factor
WHO	World Health Organization

Chapter I – Introduction

1.1 Gestational diabetes mellitus (GDM)

1.1.1 Definition and pathophysiology

For many years, gestational diabetes mellitus (GDM) was defined as any degree of glucose intolerance that was first recognized during pregnancy [13], regardless of whether the condition may have antedated the pregnancy or persisted after the childbirth. This definition facilitated a uniform strategy for detection and classification of GDM, but it was limited by imprecision. The ongoing epidemic of obesity and diabetes has led to more type 2 diabetes (T2D) in women of childbearing age, resulting in an increased number of pregnant women with undiagnosed T2D [14]. Therefore, GDM classification has been recently revised and consists of a carbohydrate intolerance of any degree diagnosed in the second or third trimester of pregnancy, that is not clearly overt diabetes [15]. Risk factors for gestational diabetes include certain ethnicities, obesity, a personal history of GDM, a family history of T2D, maternal age, polycystic ovary syndrome, a sedentary lifestyle and exposure to toxic factors [16]. According to the American Diabetes Association (ADA), GDM complicates approximately 7% of all pregnancies, whereas its total incidence is estimated to be up to 17.8% depending upon the diagnostic criteria used and the demographic characteristics of the population [1]. The greatest rises in prevalence are predicted to occur in India, China, Latin America and the Middle East [17].

GDM is closely associated with T2D, as they share many key pathophysiological characteristics; namely a relative insufficiency of pancreatic β-cell function and insulin resistance. During pregnancy, insulin resistance is increased due to the production of placental hormones, such as estrogens, cortisol and human placental lactogen (HPL), and cytokines including tumor necrosis factor α (TNF-α), which antagonize insulin action [18]. This increase is additional to the insulin resistance that occurs due to genetic susceptibility and/or a suboptimal lifestyle. In the event there is adequate release of insulin by the maternal pancreas, normoglycemia is preserved and the embryo is not affected. However, when insulin release is insufficient, hyperglycemia occurs and an excess amount of glucose is transferred via the placenta to the embryo while maternal insulin cannot pass the placental barrier causing fetal hyperglycemia. As a consequence the fetal pancreas produces more insulin to counter the increased glucose levels leading to hyperinsulinemia and excessive fetal growth (macrosomia) [19]. Figure 1.1 shows the basic concepts of GDM pathophysiology.

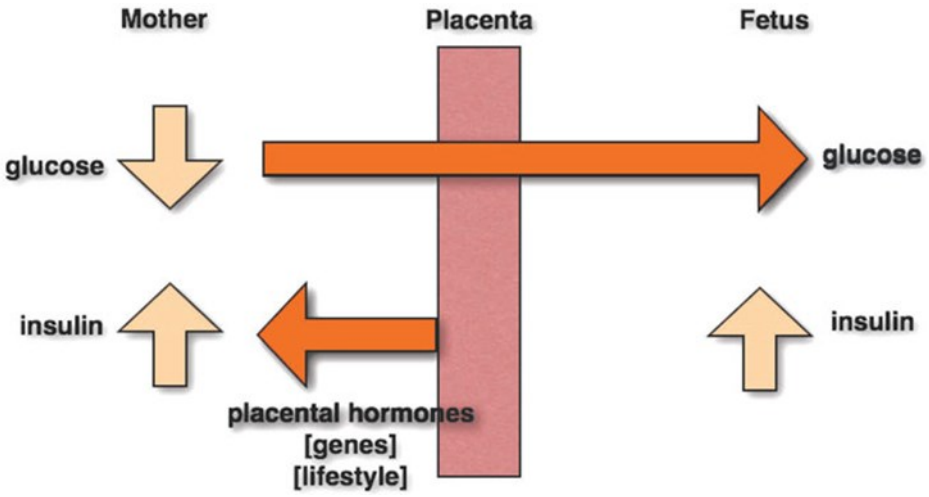


Figure 1.1: Pathophysiology of gestational diabetes mellitus
During pregnancy placental hormones, genetic susceptibility and/or a suboptimal lifestyle lead to an increase of maternal insulin resistance and hyperglycemia. Maternal glucose can then transfer to the fetus through the fetoplacental circulation, while maternal insulin is unable to pass the placental barrier. Maternal hyperglycemia consequently stimulates fetal hyperinsulinemia to counter the extra glucose. The high insulin level in the fetus stimulates growth which results in fetal macrosomia [19]. The schematic is adapted from [20]

GDM usually reverses after delivery, but altered glucose homeostasis harms the mother and can lead to health consequences in the fetus. The short-term complications for a mother with GDM include pre-eclampsia, polyhydramnios and caesarean section. Similarly, the main short-term fetal and neonatal complications include perinatal mortality, macrosomia, obstetric trauma, hypoglycemia, hyperbilirubinemia, hypocalcemia and cardiac dysfunction [21,22]. Additionally, GDM is associated with long-term complications for both the mother and child, including T2D and cardiovascular diseases (CVD) [23].

1.1.2 GDM and long-term maternal outcomes

It is well established that GDM is associated with an increased risk of developing T2D postpartum, occurring as a consequence of insulin resistance developed during pregnancy [24]. For the majority of women who go on to develop T2D, GDM does resolve immediately postpartum, with the loss of placental hormones and the reduction in circulating cytokines, but their glucose tolerance worsens with time, such that after 5 years 13% of such woman have developed T2D [25]. In an Australian retrospective study of 5470 GDM patients and 783 control subjects (follow up between 1971 and 2003),

the risk of developing diabetes increased with time of follow-up and was 9.6 times greater for patients with GDM [26].

GDM is also a risk factor for CVD events. In a large population-based study in Ontario, Canada, women who had GDM in pregnancy compared with a matched control group were at higher risk of CVD events with an odds ratio of 1.71 (95% CI 1.08 - 2.69) [27]. When adjusted for the risk of development of T2D, this ratio was no longer significant because the considerable part of increased CVD risk was attributable to progression to T2D. Therefore, a diagnosis of GDM for each woman provides an opportunity for intervention to reduce her risk of future T2D and cardiovascular complications.

1.1.3 Fetal programming and GDM long-term outcomes for the offspring

Our knowledge of the role of maternal diabetes in fetal programming started in 1952 with the "Pedersen hypothesis". Pedersen proposed that elevated maternal glucose crossed the placenta resulting in hyperinsulinemia and excessive fetal growth, thus leading to fetal macrosomia [19]. In 1980, Freinkel expanded upon the Pedersen hypothesis and proposed that excesses of mixed "fuels" including glucose, amino acids, lipids, ketones, and possibly altered concentrations of other nutrients, induce "teratogenesis". Importantly, Freinkel suggested that the teratogenic effects resulting from exposure to elevated levels of maternal mixed nutrients, and the timing of such exposures, might have profound and long-term consequences for the fetus [28]. Some years later epidemiological studies on birth and death records by David Barker and colleagues led to the idea that babies who are born lighter and survived infancy might have an increased risk of developing coronary heart disease later in life. This led to the "Barker hypothesis" or "fetal programming hypothesis" which states that adverse intrauterine environments will have long-term effects on adult health which includes an increase in incidence of T2D, hypertension and coronary heart disease [29]. The Dutch "Hunger Winter" is one of the earliest and best examples of "fetal programming" during World War II, when shortages in food supply caused famine in western Netherland's population. The pregnancies during that period were affected by "foetal starvation" which ultimately had long-term effects on the health of the newborn [30]. What is unique about the Dutch Famine as an experimental study on the effects of maternal malnutrition, is that the population was strictly circumscribed in time and place and the

sudden onset and relief of the famine was imposed on a previously well-nourished population [31].

This concept of fetal programming of adult metabolic diseases is well supported by several studies and thus now widely accepted. Discordant human siblings born before and after the development of GDM provided compelling evidence that these later life phenotypic consequences are caused by the diabetic uterine environment [2]. In longitudinal studies of the Pima Indians from Arizona, a population that has an extremely high prevalence of obesity and T2D, diabetes during pregnancy does increase the incidence of T2D in the offspring, principally at a young age [2,4]. Moreover an association was found between maternal diabetes and age at offspring's diagnosis of T2D in the multiethnic SEARCH for diabetes in youth study [3]. This evidence supports the concept that exposure to hyperglycemia during fetal development increases the subsequent risk of diabetes and cardiovascular complications later in life. The molecular mechanisms underlying this developmental programming of metabolic and cardiovascular diseases are still largely unclear. However, in addition to genetics, epigenetic mechanisms appear to play a key role [32].

1.1.4 Diagnosis and screening

Even though GDM is a common disorder in pregnancy, it has been difficult to compare its frequency among various populations and estimate its global incidence, due to the lack of uniform diagnostic criteria [33].Over the last few decades, different diagnostic criteria have been applied according to different rationales as presented in Table I [34]. All these criteria are based on fasting or non-fasting maternal glucose concentrations, most usually by means of an oral glucose tolerance test (OGTT) [35–37]. As the most important issue in GDM is the development of embryonic, neonatal or maternal complications, maternal glucose concentrations need to be used to predict the development of complications with the highest possible sensitivity and specificity. However, the adoption of a low glucose threshold results in overdiagnosis, as many women who are not likely to develop complications will be diagnosed as having GDM. By contrast, the adoption of a high threshold results in underdiagnosis, as numerous women who would go on to develop complications will be diagnosed as not having GDM. Even the adoption of an intermediate threshold will result in a lower but serious risk for over- and underdiagnosis. Thus, the definition of GDM by means of maternal glucose concentrations constitutes a difficult challenge.

The Hyperglycemia and Adverse Pregnancy Outcomes (HAPO) study attempted to tackle this challenge by assessing 25,505 pregnant women from 15 countries during the third trimester of gestation [38]. The study pointed out that there is no specific threshold for maternal serum glucose over which the chance of developing maternal or neonatal complications increases significantly. By contrast, the correlation between the degree of glycemia and the probability of adverse outcomes (e.g. neonatal birth weight >90th percentile, primary caesarean section, neonatal clinical hypoglycemia, cord-blood C-peptide concentrations >90th percentile) is linear [38].

Based on the data from the HAPO study, in 2010 the International Association of Diabetes and Pregnancy Study Groups (IADPSG) decided to set the threshold at an odds ratio of 1.75 for developing specific complications, specifically an increase in neonatal fat mass, fetal macrosomia and cord C-peptide concentrations >90 percentile, compared with mean glucose concentrations. This odds ratio corresponds to a fasting plasma glucose of 92 mg/dl, or 180 mg/dl and 153 mg/dl after an OGTT with 75 g of glucose at 1 and 2 hours, respectively (Table I) [39]. In other words, a diagnosis of GDM set by the IADPSG criteria means that the specific woman has a 75% increased odds (odds ratio 1.75) of developing complications as compared to a woman with mean glucose concentrations. According to the same criteria, if a woman has a fasting glucose of more than 126 mg/dl, a random glucose of more than 200 mg/dl or a glycosylated hemoglobin (HbA1c) of more than 6.5%, then a diagnosis of pre-existing diabetes mellitus (DM) has to be made [40]. The IADPSG criteria have a number of advantages. They represent a unique opportunity for uniformity in GDM diagnosis, are simple and can be compared with similar criteria for DM diagnosis in the non-pregnant state. On the other hand, they have been developed based on observational studies of GDM complications and cannot necessarily be used as treatment thresholds. In addition, they increase the GDM prevalence from 5-6% to 16%, being more inclusive than older criteria [37,41].

		Plasma glucose concentrations thresholds (mg/dl)			
Organization	OGGT glucose load	Fasting	1-hour	2-hours	3-hours
ADA*	100g	95	190	155	140
ACOG*	100g	105	180	165	145
WHO^	75g	126	-	140	-
IADPSG^	75g	92	190	153	-

Table I: GDM diagnostic threshold values from various organizations
*Diagnose GDM if two or more glucose values equal or exceed the threshold values, ^Diagnose GDM if one or more glucose values equal or exceed the threshold values. ADA (American Diabetes Association), ACOG (American Congress of Obstetricians and Gynecologist, WHO (World Health Organization), IADPSG (International Association of the Diabetes and Pregnancy Study Group.

Regarding screening for GDM, the latest guidelines drawn up by the Endocrine Society (ES) are the first to recommend universal testing for overt DM in early pregnancy. A fasting plasma glucose, HbA1c or a random plasma glucose at the first prenatal visit (before 13 weeks of pregnancy or as soon as possible thereafter) is recommended for those women not known to already have DM. In the event of overt DM, a second test is recommended on another day to confirm the diagnosis. In all pregnant women in whom no overt DM or GDM has been diagnosed, a 2-hour 75-g OGTT should be performed at 24 to 28 weeks of pregnancy [42].

1.1.5 Treatment of GDM

The beneficial effect of early diagnosis and treatment of GDM or mild carbohydrate intolerance during pregnancy has been recently demonstrated by two large randomized clinical trials. The Australian Carbohydrate Intolerance Study in Pregnant Women, established that GDM treatment in the form of dietary advice, blood glucose monitoring, and insulin therapy, as required for glycemic control, reduces serious perinatal complications and may also improve health-related quality of life [21]. Also, the American

Maternal-Fetal Medicine Units Network study provided further compelling evidence that among women who have GDM and normal fasting glucose levels, treatment that includes dietary intervention and insulin therapy, as necessary, reduces rates of fetal overgrowth, cesarean delivery, and preeclampsia [43]. Accordingly, the primary intervention recommended to women diagnosed with GDM is dietary counseling in combination with physical activity and self-monitoring of blood glucose [44,45]. If these measures are insufficient in terms of achieving optimal glycemic control, subcutaneous insulin administration is the therapy of choice as insulin does not cross the placenta and is therefore considered harmless to the fetus. However insulin is relatively expensive and difficult to administer, it requires education to ensure safe administration and moreover it is associated with an increased risk of hypoglycemia and weight gain. The use of safe and effective oral anti-hyperglycemic agents may therefore offer advantages over insulin but has not yet been formally approved for GDM therapy in all countries [46]. In this context, two large randomized controlled trials were performed to test the effectiveness and safety of metformin [47] and glyburide, a sulphonylurea that acts as an insulin secretagogue. [48] From these studies, the authors concluded that both metformin and glyburide, alone or with supplemental insulin, were not associated with increased perinatal complications as compared to insulin. More studies show that both metformin and glyburide have been increasingly and safely used in the treatment of GDM [49]. However, both medications can cross the placenta and given the growing evidence of epigenetic fetal programming *in utero*, the administration of drugs potentially affecting fetal metabolism is of major concern. As long term follow-up data on both mother and offspring are lacking, oral anti-hyperglycemic agents should be used with caution.

1.2 Maternal hyperglycemia and fetal endothelial dysfunction

1.2.1 Biochemical and cellular signaling underlying diabetic vascular complications

Hyperglycemia has been shown to be the major risk factor for the development of diabetic complications due to its long-term deleterious effects on various tissues and a particular subset of cell types. Indeed most cells are able to reduce the transport of glucose inside the cell when they are exposed to hyperglycemia, so that their internal glucose concentration remains constant. In contrast, the cells damaged by hyperglycemia are those that cannot do this efficiently [50,51]. Thus, diabetes selectively damages cells, like endothelial cells, mesangial cells, neurons and Schwann cells in peripheral nerves, whose glucose transport rate does not decline rapidly as a result of hyperglycemia, leading to high glucose concentrations inside the cell.

High glucose can lead to the activation of several cellular pathways, including increased oxidative stress [52–54], enhanced flux into the polyol and hexosamine pathways [55], activation of Protein Kinase C (PKC) [56] and increased formation of advanced glycation end products (AGEs) [57] as shown in Figure 1.2. Studies in mesangial, endothelial, and other cell types have associated hyperglycemic activation of these pathways to increased mitochondrial superoxide anion formation (O^{2-}) and associated oxidative stress [58], which can ultimately lead to increased formation of extra cellular matrix (ECM) proteins in the kidney, contributing to renal dysfunction [59,60].

In addition, high glucose can activate the pro-inflammatory transcription factor NF-kB, resulting in increased inflammatory gene expression in part through oxidative stress, AGEs, PKC, and MAPKs [61,62]. Inflammation can also lead to the acceleration of diabetic complications due to detrimental effects on vascular cells and insulin resistance in T2D. Furthermore, insulin resistance has been attributed to increased free fatty acids which, in conjunction with hyperinsulinemia, lead to dyslipidemia [63]. Therefore, hyperglycemia and dyslipidemia can alter the expression of inflammatory and other pathological genes and proteins related to the development of endothelial dysfunction [64], which precedes the pathogenesis of vascular complications in diabetes.

Similar to other forms of diabetes, GDM is associated with structural and functional alterations in various tissues including endothelial dysfunction. It is believed that a dysfunctional endothelium could lead to impaired vasodilation, increased leukocyte adhesion to the vascular wall and platelet aggregation, and impaired angiogenic

properties. Endothelial dysfunction in GDM is likely to be at least partially a consequence of hyperglycemia which induces changes in the proliferation and inflammatory responses of endothelial cells (ECs) *in vitro*. Decreased proliferation of human umbilical vein endothelial cells (HUVECs) from normal pregnancies exposed to elevated glucose have been extensively studied and attributed to increased cell death [65]. Moreover HUVECs isolated from gestational diabetes pregnancies presented enhanced monocyte adhesion and altered L-arginine transport and nitric oxide (NO) synthesis probably due to an altered uptake and metabolism of adenosine [66,67].

Fetal endothelial dysfunction is involved in the abnormal vascular development caused by GDM, and it might be responsible for the increased cardiovascular risk and incidence of T2D observed later in life in the offspring from GDM mothers [68,69].

The mechanisms that link hyperglycemia to fetal endothelial dysfunction and cardiovascular complications in adulthood is still largely unknown and different explanations have been proposed including the existence of a “metabolic memory”.

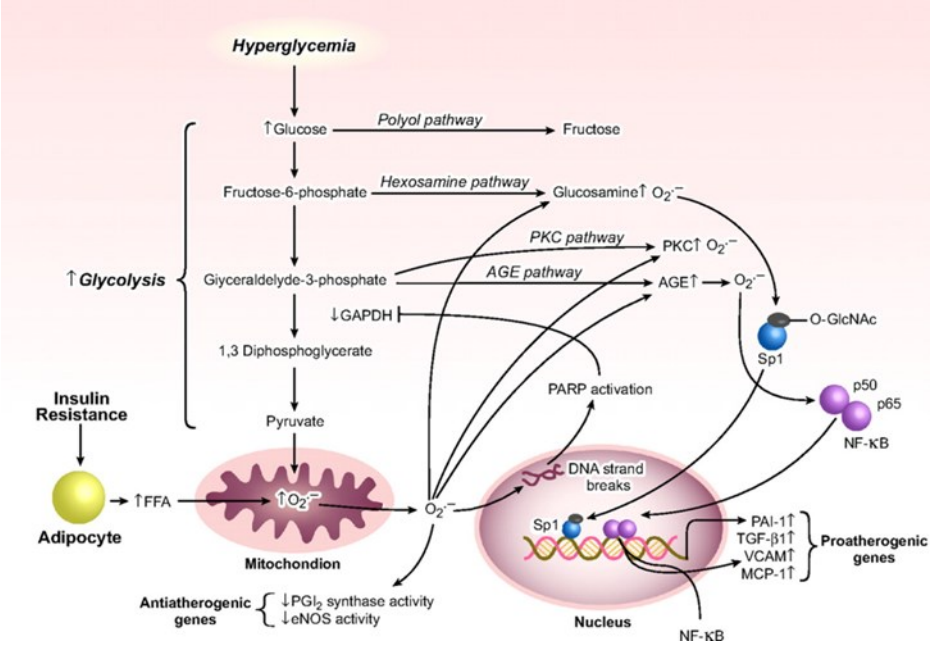


Figure 1.2: Biochemical and cellular signaling activated by hyperglycemia
Insulin resistance and hyperglycemia increase mitochondrial O^{2-} production which activates atherogenic signaling pathways. Overproduction of mitochondrial O^{2-}, results in DNA strand breaks and activation of poly-ADP-ribose polymerase (PARP). PARP ribosylates and inactivates glyceraldehyde-3-phosphate dehydrogenase (GAPDH). The upstream metabolites of the interrupted glycolytic pathway are processed through polyol, hexosamine, PKC, or AGEs pathways. Activation of transcription factor NF-κB, downstream of the AGE pathway, induces transactivation of vascular cell adhesion molecule-1 (VCAM-1) and monocyte chemoattractant

protein-1 (MCP-1). Increased flux of FFAs, released from insulin-resistant adipocytes, also activates hexosamine, PKC, and AGE pathways. In addition, FFA-induced excess mitochondrial O^{2-} production inactivates anti-atherogenic enzymes such as prostacyclin (PGI_2) synthase and eNOS. The illustration is adapted from [70].

1.2.2 "Metabolic memory" and GDM vascular complications

The results of more than one clinical trial on T1D and T2D patients have demonstrated that the development of diabetic complications persisted even after the achievement of glycemic control, suggesting the existence of a "metabolic memory" dependent from prior exposure to hyperglycemia. T1D patients in the Diabetes Control and Complications Trial (DCCT) under intensive insulin therapy were found to have delayed progression of nephropathy, retinopathy, and neuropathy compared with patients under conventional therapy [71]. The large benefits of the intensive therapy led to the premature termination of the DCCT so that all patients could be placed on intensive insulin therapy and followed long-term under the subsequent Epidemiology of Diabetic Complications and Interventions Trial (EDIC). In line with the DCCT findings, long-term follow-up in the EDIC trial demonstrated that patients who were originally in the intensive treatment group during the DCCT and continued on intensive therapy for the EDIC trial had significantly slower progression of key diabetic microvascular complications in comparison to patients who were in the conventional treatment group during DCCT, even though they were placed on intensive therapy [5]. More recently, patients in the continuous intensive treatment group since the beginning of the trials were found to also have better outcomes for macrovascular complications including stroke, nonfatal heart attack, or death by cardiovascular disease [5], as well as decreased progression of coronary artery calcification and intima-media thickness, both of which are associated with atherosclerosis [8].

Long-lasting benefits of glycemic control have also been seen in T2D patients. In this context the United Kingdom Prospective Diabetes Study (UKPDS) found that lower fasting plasma glucose at the time of diagnosis correlated with decreased cardiovascular risk [72,73]. In addition, the Steno-2 Study found a decreased risk of cardiovascular events and death following intensive multifactorial therapy including tight glycemic control [74].

Overall, the findings from these major clinical trials demonstrate that the exposure to prolonged hyperglycemia leaves a long-lasting impression on vascular cells and progressively induces the development of vascular complications, which persist after

glycemic control is achieved. However, the same studies also demonstrated that good glycemic control can delay the onset of diabetic vascular complications. Both lines of evidence are compatible with an underlying implication of epigenetic mechanisms. Indeed, epigenetic factors allow cells and organisms to respond to changing internal and environmental stimuli and additionally confer the ability of the cell to memorize these environmental situations.

1.2.3 Models of metabolic memory

Experimental models provide an opportunity to study the molecular mechanisms responsible for metabolic memory in order to design better therapies for diabetic patients. Recent research has demonstrated the presence of metabolic memory in several animal and cell culture models. Early studies in dogs found that there was a persistence of retinal complications even after reversal of hyperglycemia [75]. Similar results with diabetic rats showed that islet transplantation after 12 weeks of diabetes could not reverse the progression of retinopathy compared with the same surgical treatment after 6 weeks of diabetes [76]. Moreover several studies in streptozotocin (STZ)-induced diabetic rats showed that establishment of glycemic control after a short period of hyperglycemia had protective effects on NO levels, lipid peroxides, and other parameters in the retina. However, reinstitution of physiological glucose concentrations after prolonged hyperglycemia failed to reverse increases in oxidative stress, NF-kB activity, as well as inflammation, and this was attributed to metabolic memory [73,77].

The presence of a metabolic memory has also been demonstrated in vascular cell models. Early *in vitro* studies with endothelial cells cultured in high glucose showed continued increased expression of genes encoding fibronectin and collagen ECM proteins even after normalization of glucose levels [78]. A more recent endothelial cell model of metabolic memory showed that even a short-term exposure to high concentrations of glucose resulted in sustained increases in the expression of the NF-kB p65 subunit, inflammatory genes, and oxidative stress that persisted even after a return to normal glucose levels [79,80]. Finally, other recent reports demonstrated the persistence of oxidative stress for up to 1 week after glucose normalization and that antioxidants or NADPH oxidase inhibitors partially blocked the high glucose effects [81].

Together, these results suggest a metabolic memory of vascular dysfunction arising from acute hyperglycemic spikes or prior chronic exposure to high glucose conditions. In addition, these experimental models confirm that strict control of glucose levels is

essential to slow down the progression of diabetic complications. Importantly, they also suggest that oxidative stress, along with epigenetic mechanisms, may be responsible for the sustained metabolic memory over time through multiple cell divisions.

1.3 Role of epigenetic factors in GDM vascular complications

1.3.1 Epigenetics and transcriptional regulation of gene expression

Epigenetics refers to heritable changes in the phenotype that do not involve changes in the genotype and include mainly two mechanisms: DNA methylation and histone tails modification [6]. In the promoter regions, DNA methylation that typically occurs at CpG islands reduces gene expression by blocking the binding of transcription factors or promoting chromatin packing. Post-translational modifications that occur on the histone tails include mainly acetylation, methylation, and phosphorylation [7]. Along with DNA methylation, these epigenetic modifications make up an additional level of gene regulation or code that can be altered without altering the DNA code itself. In addition, the numerous combinations of epigenetic modifications allow for flexibility of the chromatin and can affect recruitment and binding of various DNA and histone binding complexes that recognize specific combinations of chromatin marks, as shown in Figure 1.3. Histone binding complexes often contain other chromatin-modifying proteins that can further change the chromatin structure. In this context, histone acetyltransferases (HATs) mediate histone lysine acetylation, a chromatin mark generally associated with euchromatin formation and activation of gene transcription. Histone deacetylases (HDACs), on the other hand, mediate the removal of lysine acetylation and are found to be components of repressor complexes [82]. Overall, histone acetylation can occur quite rapidly and is quite dynamic.

By contrast, histone methylation is considered to be more stable and long lasting. Histone methylation occurs on both lysine and arginine residues and is associated with either gene activation or repression depending on which residue is modified [7]. The SET domain-containing family of histone methyltransferases (HMTs), which is named for a conserved sequence motif found in three Drosophila proteins, Suppressor of Position Effect Variegation, Enhancer of Zeste and Trithorax, are involved in regulating lysine methylation [83]. Lysine methylation can be quite complex since lysine residues can be mono-, di-, or trimethylated by specific HMTs which usually methylate only one particular lysine residue. Specifically, histone H3 lysine 4 methylation (H3K4me) is typically associated with gene activation while H3K9me, is generally associated with gene repression. In addition, there are several other lysine residues, including H3K27, H3K36, and H3K79, that can be methylated to various degrees by different HMTs, leading to altered gene expression [84].

The exciting discovery of the first histone demethylase (KDMs), lysine demethylase 1 (LSD1) which specifically removes H3K4me [85] and H3K9me marks [86], demonstrated that histone lysine methylation can also undergo dynamic regulation. Numerous KDMs have since been identified with specificities for different histone lysine residues [87]. In the context of diabetes, a recent report demonstrated that histone demethylase JHDM2A is associated with obesity and affects genes related to metabolism in rodent models [88].

According to an early definition, epigenetics is associated with chromatin changes which are transmitted from parents to offspring. However, this concept has been revisited and it is now suggested that epigenetic changes have a long lasting effect, which can be transmitted at cell division, but that are not necessary perpetual. In other words, the epigenetic modifications once written, can still be diluted and possibly erased over time under particular circumstances, such as with the use of drugs or lifestyle changes [5]. The concept of a changeable epigenetic status is important because it confers therapeutic hope at different stages of prenatal and postnatal life.

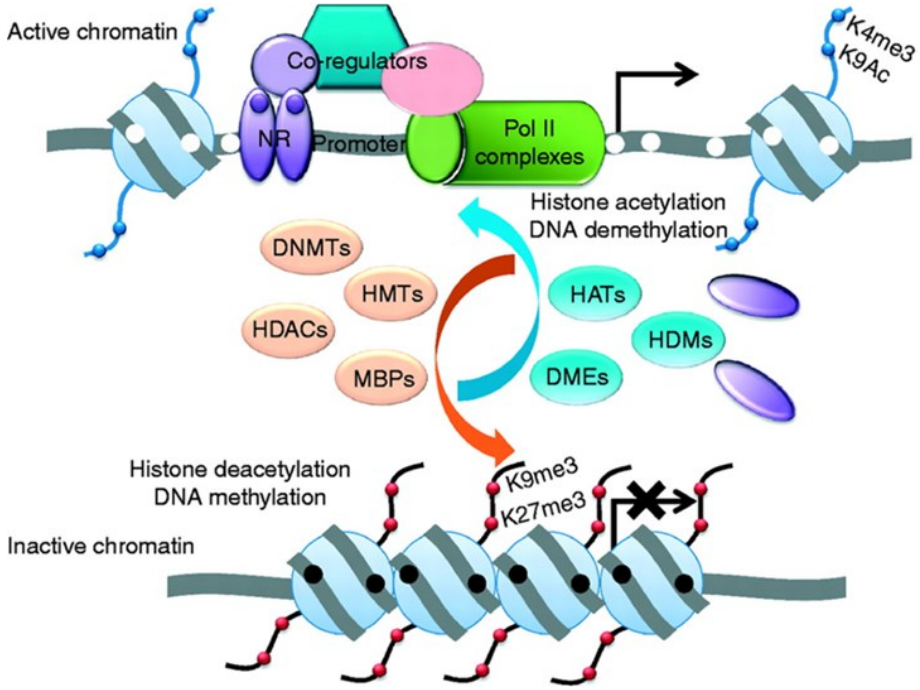


Figure 1.3: Regulation of chromatin by histone modifications
The two major epigenetic modifications are DNA methylation and histone modifications which regulate the active or inactive chromatin state. Hypermethylation of the promoter is associated with transcriptional silencing due to the loss of affinity for transcriptional factors such as the nuclear receptor (NR) and accessibility by the transcriptional machinery. The inactive chromatin has increased affinity for methylated DNA-binding proteins (MBPs), which further recruit histone

deacetylases (HDACs), DNA methyltransferases (DNMTs), histone methyltransferases (HMTs) and other corepressors. Methylated promoters are associated with unique repressive histone marks, which classically include trimethylation of histone 3 on lysine 9 (H3K9me3), and trimethylation of histone 3 on lysine 27 (H3K27me3). By contrast, unmethylated promoters are associated with gene transcription. They have increased affinity for histone acetylases (HATs), histone demethylases (HDMs), DNA demethylases (DMEs), and histone marks associated with active chromatin, including acetylation of histone H3 on lysine 9 (H3K9Ac) and trimethylation of histone H3 on lysine 4 (H3K4me3). The illustration is adapted from [7].

1.3.2 Transmission of epigenetic modifications

Epigenetic marks are transmitted through multiple cell cycles. While much is known about the epigenetic inheritance of DNA methylation, the exact mechanisms responsible for the stable transmission of histone modifications are less well understood. Replication-associated transmission, histone variants, and chromatin remodeling complexes are some of the factors that have been implicated.

Methylation of histone lysine residues has been shown to be transmitted through replication where the methyl-CpG binding protein recruits the HMT SETDB1 to chromatin during replication to methylate newly-deposited histones and thus coupling the transmission of H3K9 methylation with DNA methylation [89]. Evidence has also shown that the long-term silencing Polycomb complex remains bound to chromatin during replication, possibly binding more than one nucleosome and allowing nucleosomes to maintain contact with chromatin even as the replication fork passes through. Alternatively, the complex could interact directly with the replication machinery [90]. Another study demonstrated that the Polycomb repressor complex 2 containing the HMT EZH2 can bind H3K27me3 modifications at sites of ongoing replication, which would then allow transmission or copying of the parental H3K27me3 marks to the new histones deposited on the daughter strand [91]. Interestingly the Polycomb complex family has been recently found to play a role in the epigenetic regulation of pancreatic cell regeneration associated with diabetes [92].

Together, these results highlight the need for further investigation into the mechanisms by which diabetes-induced epigenetic changes might be stably transmitted through cell replications to establish a transcriptional or metabolic memory associated with diabetic complications.

1.3.3 Role for microRNAs in epigenetic regulation

One of the emerging areas of research involves the post-transcriptional regulation of gene expression through a recently discovered group of small RNAs, the microRNAs (miRNAs). MiRNAs are single-stranded, non-coding RNAs of 19-25 nucleotides that normally bind the 3'-untranslated region of target mRNAs, leading to either translational repression or RNA degradation [93].

MiRNAs produced via the canonical pathway are transcribed in the nucleus by RNA polymerase II into primary miRNAs (pri-miRNAs) that are several hundred nucleotides in length. Subsequently, the microprocessor complex, which consists of Di George syndrome Critical Region gene (DGCR8) and the nuclease Drosha, cleaves the pri-miRNAs, with a stem-loop structure, into miRNA precursors (pre-miRNAs) of approximately 60 to 70 nucleotides. In the non-canonical miRNA pathway, miRNAs are transcribed directly as endogenous short hairpin RNAs (endo-shRNAs) or derived directly by splicing from introns (mirtrons) [94]. Next, exportin-5 transports the pre-miRNAs from the nucleus to the cytoplasm via a RAN-GTP-dependent process. The pre-miRNAs are further processed in the cytoplasm by RNase Dicer in association with Transactivation Response RNA Binding Protein (TRBP) to final miRNA duplexes of 19-25 nucleotides. Finally, the mature single-stranded miRNAs are generated and incorporated into the RNA-Induced Silencing Complex (RISC) and are ready to interact with specific mRNA targets [93]. The miRNAs biogenesis pathways are depicted in Figure 1.4.

MiRNAs provide a rapid but reversible system of gene regulation, which also allows the cell/tissue/organism to respond to environmental stimuli without changing the DNA sequence itself. MiRNAs have been identified as negative regulators in various pathways, targeting signaling molecules, transcription factors, and numerous other enzymes and proteins. There is also the potential for miRNAs to target chromatin-modifying enzymes which in turn could also affect transcription and expression of miRNAs [95]. Therefore, miRNAs may themselves be epigenetically regulated.

Recent findings have demonstrated a critical role for miRNAs in various diseases. They have been found to play key roles in proliferation, differentiation, development, and in cancer, where they can act as oncogenes or tumor suppressors [93,96]. MiRNAs are also associated with the regulation of genes relevant to insulin secretion, cholesterol biosynthesis, fat metabolism, adipogenesis and angiogenesis, crucial pathways in the pathogenesis of diabetes and its vascular complications [97,98]. The role

of miRNAs and their potential relationships to epigenetic mechanisms in diabetic complications are currently an area of great interest both as a means for understanding the molecular pathways leading to these complications and for discovering new potential therapeutic targets.

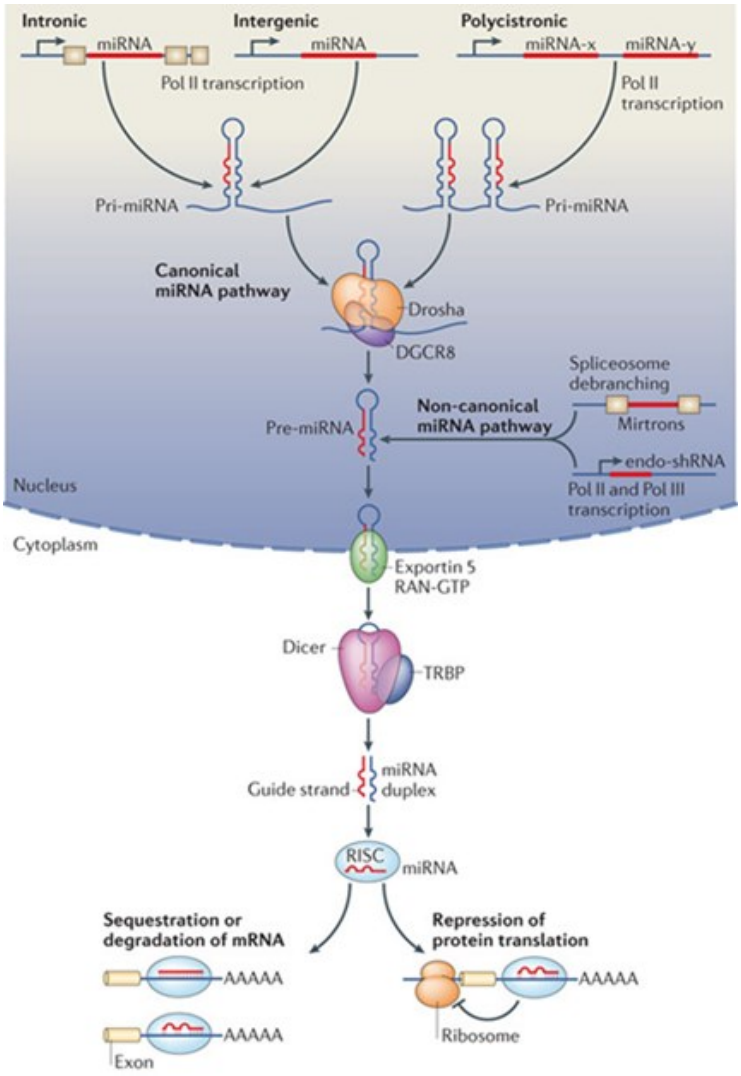


Figure 1.4: MiRNA biogenesis pathways
MiRNAs, produced via the canonical pathway are transcribed from genomic DNA in the nucleus as long primary miRNAs (pri-miRNA) by RNA polymerase II. The pri-miRNA transcript forms a stem-loop structure that is recognized and processed by Drosha in association with DGCR8 into a precursor miRNA (pre-miRNA). In the non-canonical miRNA pathway, miRNA are transcribed directly as endogenous short hairpin RNAs (endo-shRNAs) or derived directly by splicing from introns (mirtrons) [94]. The pre-miRNA is then exported to the cytoplasm by exportin 5 and RAN-GTP-dependent process. In the cytoplasm, pre-miRNA is further processed by RNase activity of Dicer and Transactivation Response RNA-Binding Protein (TRBP) complex to form the mature double-stranded ~22 nucleotide miRNA. The mature miRNA is then incorporated into the RISC

complex which mediates small interfering RNA silencing by degrading the target mRNA or interfering with translation. The illustration is adapted from [97]

1.3.4 MiRNAs as novel regulators of endothelial function

MiRNAs play a central role in endothelial function regulation. Elimination of most endothelial miRNAs by Dicer knockdown in ECs inhibits proliferation and tube formation *in vitro* [99]. Moreover, Dicer knockout mice have impaired blood vessel development [100]. These findings suggest that miRNAs are essential for the maintenance of vascular homeostasis.

The first large analysis of miRNA expression in ECs was carried out in HUVECs and identified 15 highly expressed miRNAs and some of their angiogenic mRNA targets (Flt-1, Nrp-2, Fgf-R, c-Met, and c-kit), according to prediction algorithms [101]. Additional studies also profiled the expression of miRNAs in ECs [102]. The highly expressed miRNAs that were common in at least two of the three studies included miR-15b, 16, 20, 21, 23a and 23b, 24, 29a and 29b, 31, 99a, 100, 103, 106, 125a and 125b, 126, 130a, 181a, 191, 221, 222, 320, let-7, let-7b and let-7c [99,101].Several miRNAs have also emerged as potential regulators of EC function under diabetic conditions. Wang et al. identified that high glucose levels induced miR-320 expression in myocardial microvascular ECs. Inhibition of miR-320 improved proliferation and migration, which has implications for diabetic-impaired angiogenesis [103]. More recently, expression of miR-503 was found to be increased in ECs exposed to high glucose levels *in vitro*. Consistently, miR-503 expression also increased in ECs enriched from ischemic limb muscles of STZ-induced diabetic mice [104]. Moreover, miR-503 expression was remarkably higher in the limb muscles and plasma from diabetic patients and inversely correlated with expression of cell division cycle 25A, a known target gene that controls cell cycle function. Local inhibition of miR-503 promoted vascular wound healing and blood-flow recovery in a diabetic mouse model of limb ischemia [104]. Expression of another miRNA, miR-29c, was increased in microvascular ECs exposed to hyperglycemic conditions and in the kidney from diabetic mice. Upregulation of miR-29c decreased Spry1 protein levels and promoted activation of Rho kinase, which suggests that miR-29c may play a role in kidney remodeling during diabetic nephropathy [105]. Additionally, miR-221 expression increased in ECs in response to advanced glycation end products or glucose, and its overexpression reduced c-kit expression [106].

MiR-101 is known to affect endothelial function and angiogenesis under normal glucose conditions [12] and to target the histone methyltransferase Enhancer of Zester Homologue 2 (EZH2) for inhibition [12,107–109]. However, its role in the context of diabetes is still unexplored.

1.3.5 Enhancer of Zeste Homologue 2 and its role in angiogenesis

EZH2 is a well characterized epigenetic regulator and is a member of the Polycomb-Group (PcG) proteins. PcG proteins function as transcriptional repressors that silence specific sets of genes through chromatin modification [110]. PcG proteins act together in Polycomb Repressive Complexes (PRC). In this context, PRC2 is a multi-subunit complex which includes EZH2, Suppressor of Zeste 12 (SUZ12), and Embryonic Ectoderm Development (EED). A number of other proteins, such as retinoblastoma binding proteins 4 and 7 (RBBP4/7), enhance the enzymatic function of the complex [111].

EZH2 is the catalytically active component of PRC2, which holds the evolutionarily conserved SET domain that confers its HMT activity. Specifically EZH2 trimethylates the histone H3 at lysine 27 (H3K27me3) [112]. The H3K27me3 mark subsequently recruits PRC1, leading to the propagation of the repressed state through a variety of mechanisms, including chromatin compaction and recruitment of other chromatin-remodeling enzymes, such as DNA methyltransferases [113]. PRC1 and PRC2 are shown in Figure 1.5.

Expression profiling indicated that EZH2 promotes angiogenesis in ovarian carcinoma [114] and glioblastoma cells [12,109]. Moreover, altered EZH2 expression was described to affect angiogenesis in bladder cancer cells [115], in HUVECs [116] and *in vivo*, in a mouse model of limb ischemia [117]. It was also described that EZH2 expression is regulated by miRNAs including miR-26 [10], miR-214 [11], and miR-101 [12,107–109]. On the other hand, regulatory feedback loops between EZH2 and microRNAs have been recently identified in human tumorigenesis [95,118]. In this context EZH2 has been recently proposed to regulate miR-101 in non-ECs [115,119]. The complexity of EZH2-mediated gene silencing has further increased since the recent discovery of a novel isoform of EZH2 protein that function in mammalian cells [9].

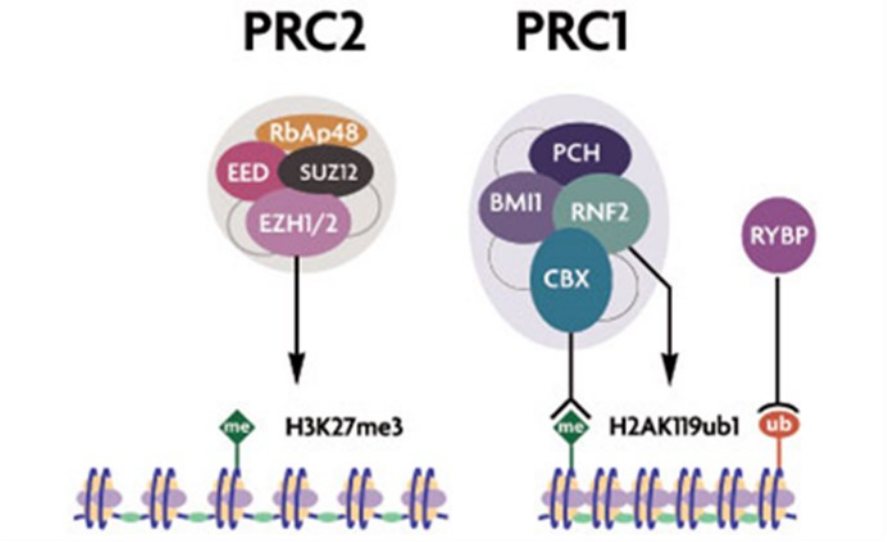


Figure 1.5: The Polycomb repressor complexes
PRC2 is a multi-subunit complex which includes EZH2, which is the catalytically active component, Suppressor of Zeste 12 (SUZ12), and Embryonic Ectoderm Development (EED). A number of other proteins, such as retinoblastoma binding proteins 4 and 7 (RBBP4/7), enhance the enzymatic function of the complex. PRC2 is recruited to chromatin and allows trimethylation of histone H3 on lysine 27 (H3K27me3) by EZH2. PRC1 is then recruited to chromatin through the recognition of H3K27me3 mark by chromobox (CBX) proteins. RNF2/RING1 homologs are E3 ubiquitin ligases for H2A, which is monoubiquitylated at lysine 119. The RYBP repressor protein recognizes H2A monoubiquitylation, contributing to transcriptional repression. The grey circular shapes in the figure depict other PRC subunits and associated proteins. The figure is adapted from http://www.activemotif.com/stem-cell-identity.

1.3.6 Enhancer of Zeste Homologue 2 and its novel isoform: EZH2-β

It has been recently shown that alternative splicing of the EZH2 locus yields two major transcriptional variants: EZH2α and EZH2β [9].

EZH2α, encoded by 20 exons, is the HMT classically associated with the function of the PRC2 complex. EZH2β, a novel isoform, skips exon 4 of EZH2α and utilizes an alternative 5′ splice donor on EZH2α exon 8/EZH2β exon 7, as presented in Figure 1.6 A. Compared with the EZH2α sequence, the shorter EZH2β shows conservation of several domains, namely the nuclear localization signals, SANT (DNA-binding domains) and the SET domain. Together, the conservation of these domains should confer this protein with the ability to localize to the nucleus and function as an HMT. Accordingly, this isoform localizes to the cell nucleus, complexes with EED and SUZ12, and binds to promoters where it increases H3K27me3 levels, all properties in common with EZH2α protein. At the protein sequence level, EZH2α and EZH2β differ by 44 amino acids, measuring 751 and 707 amino acids, respectively, as shown in Figure 1.6

B [9]. A highly similar third splice variant encoding five fewer amino acids than EZH2α has also been referred to as EZH2. Structural comparison of these closely related variants does not reveal any differences that would suggest differing function and thereby have been considered interchangeable in the literature.

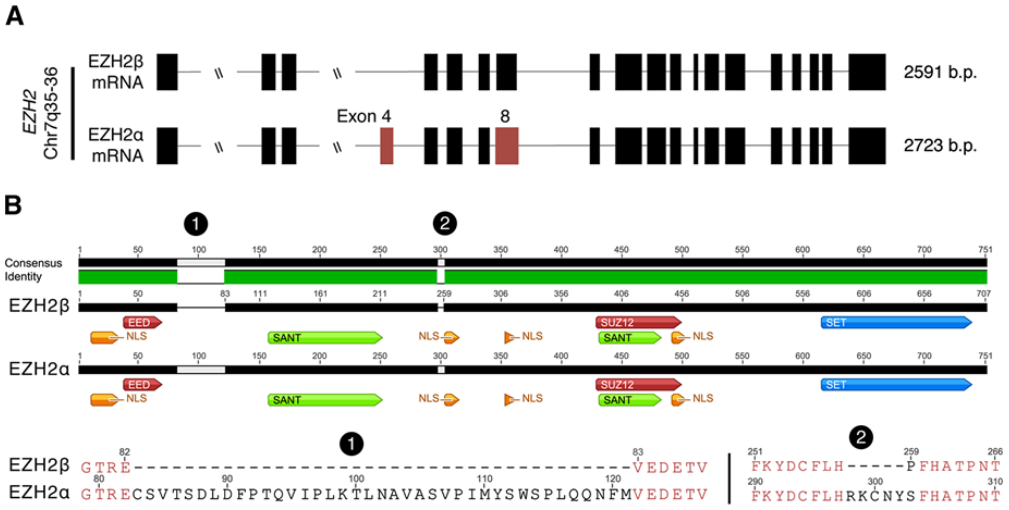


Figure 1.6: Comparative analysis of EZH2 transcriptional variants
Alternative splicing of the EZH2 locus yields two major transcriptional variants: EZH2α and EZH2β. The sites of alternative splicing events are highlighted in red on the reference isoform **(A)**. At the protein structure level EZH2α and EZH2β show the conservation of functional domains and binding sites of enzymatic co-factors, represented by different colors. Labels 1 and 2 indicate the locations of deletions in EZH2β compared with EZH2α. A comparison of the amino acid sequences highlighting the amino acid differences between the two isoforms is also presented **(B)**. The illustration is adapted from [9].

Expression profile experiments performed in pancreatic epithelial cell systems combined with adenoviral-mediated introduction of both EZH2 isoforms, using array analysis, showed that the two different isoforms can each not only regulate distinct targets but also share gene expression networks, making the regulation of transcription based on the deposition of the H3K27 histone mark more complex than previously anticipated [9].

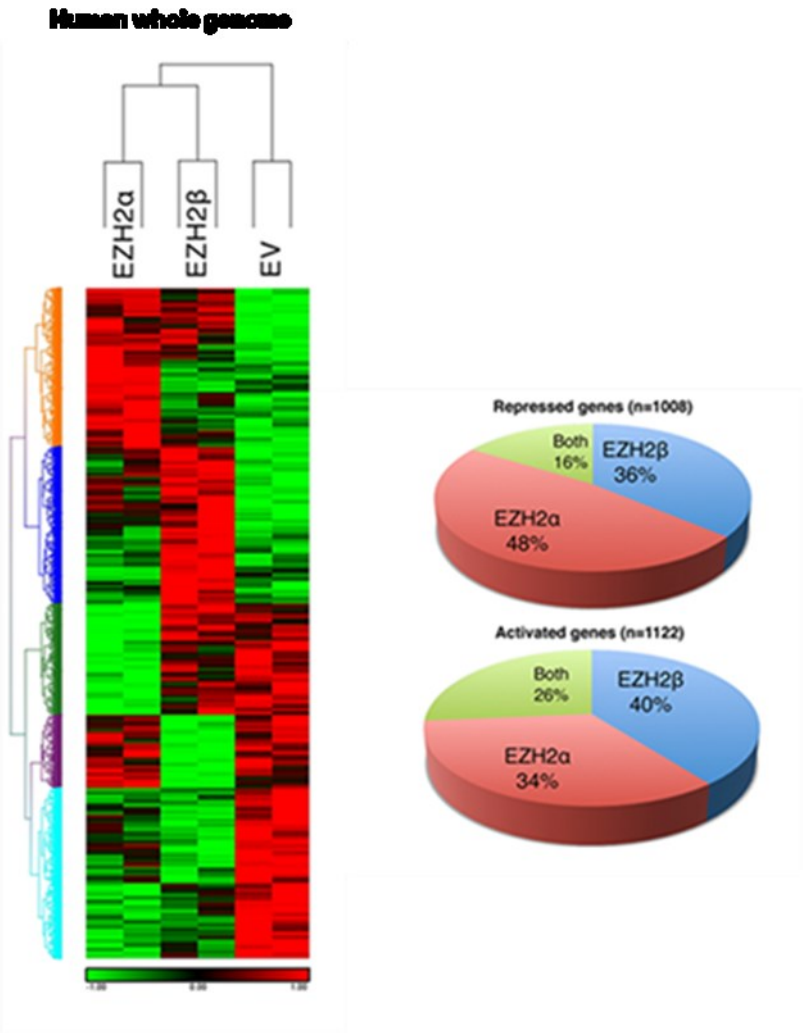


Figure 1.7: Expression patterns of EZH2α and EZH2β
Arrays analysis shows that of the 28,869 well-annotated genes assessed, 366 unique targets (36% of total repressed) are uniquely repressed by EZH2β. EZH2α-generated expression profiles display a downregulation of 480 targets (48% of total repressed). Notably, 162 targets (16% of total repressed) are repressed by both EZH2α and EZH2β. Both isoforms also induce upregulation in the expression of a significant number of targets, which may reflect indirect effects mediated by the repression of upstream regulators. Of the genes assayed, 444 (40% of total activated) are activated by EZH2β, 382 (34%) by EZH2α and 296 (26%) by both isoforms. The overall array data indicate that the novel EZH2β isoform is responsible for the expression pattern of its own unique set of genes, in addition to a group of common targets with EZH2α. The illustration is adapted from [9].

1.4 Diagnostic and therapeutic potential of miRNAs in GDM vascular complications

1.4.1 MiRNAs with diagnostic potential for vascular complications

In addition to regulating gene expression inside the cells where they are produced, several miRNAs are found in blood and other body fluids in association with proteins, exosomes and/or lipoprotein complexes as illustrated in Figure 1.8 [120,121]. The function of circulating miRNAs remains still to be elucidated. *In vitro* studies indicate that miRNAs transported by exosomes or HDL can be transferred in an active form to recipient cells thus representing a novel cell-to-cell communication mode [122].

Circulating miRNAs are very stable and resistant to treatment with ribonucleases, freezing/thawing cycles and other drastic experimental conditions [123,124]. Consequently, serum or plasma samples can be stored at −20 °C or −80 °C for up to several months without notable degradation of miRNAs, which suggests that these small RNA molecules are sufficiently robust to serve as biomarkers [125]. Circulating miRNAs have several other advantages as potential biomarkers, indeed they are found not only in blood but also in other easily accessible biologic fluids such as urine, saliva, amniotic fluid and breast milk [126]. Moreover, they can be detected by quantitative real-time PCR (qPCR), and most of them are evolutionarily conserved, which facilitates the translation of results obtained from *in vivo* animal studies to human healthcare. Although the identification of miRNAs as non-invasive biomarkers in pregnancy is still in the early stage, much progress has been made in the initial discovery phase. Some candidate miRNAs have been identified in the plasma of T2D patients, such as miR-126 [127] and miR-503 [104], and they seem to be promising biomarkers for monitoring diabetic vascular complications. GDM is associated with long-term macrovascular complications for both mother and child that can have a devastating effect on quality of life and life expectancy. The discovery of biomarkers that could be used to predict individuals at risk of serious complications such as cardiovascular disorders would enable clinicians to adapt therapeutic approaches and minimize the expected effects of the disease. However, reliable biomarkers for these long-term complications of GDM are still lacking.

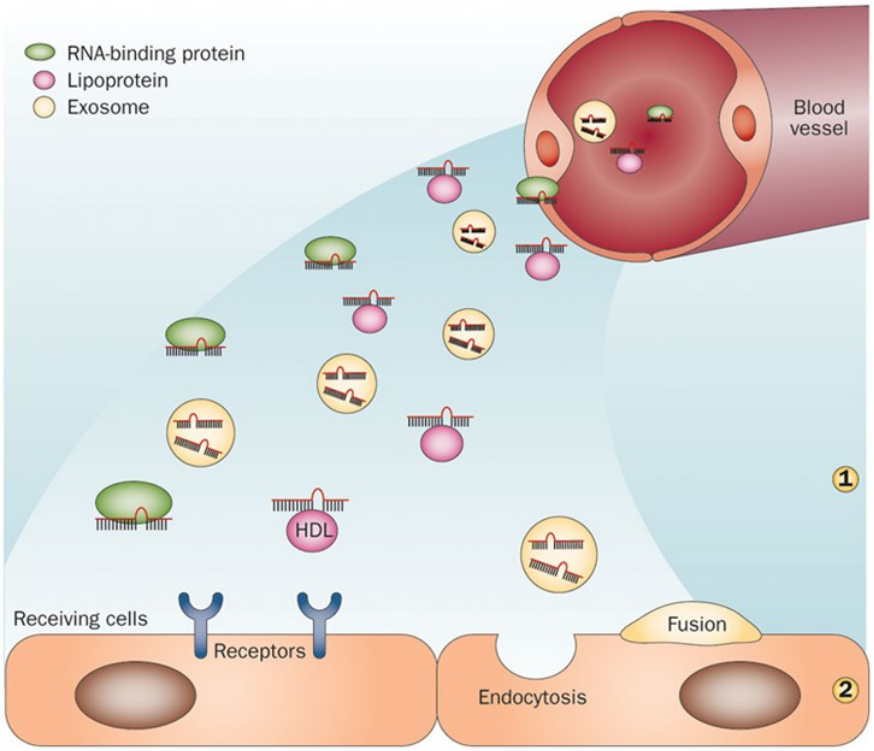


Figure 1.8: Blood and other body fluids contain active miRNAs
MiRNAs can be released by cells and are found in a stable form in body fluids. The miRNAs present in the blood are associated with protein complexes such as Argonaute-2, with HDL particles, or are transported inside membrane-bound vesicles such as exosomes (1). Circulating miRNAs can be taken up in active form through different mechanisms, including receptor-mediated capture, endocytosis or fusion of exosomes with the plasma membrane of receiving cells (2). Transfer of miRNAs between distantly located cells constitutes a potentially new communication mode. The illustration is adapted from [128].

1.4.2 MiRNAs as therapeutic targets for angiogenesis

With the increasing characterization of miRNAs in numerous diseases, the field of miRNA therapeutics is emerging. MiRNA-based therapeutics involves modulation of disease-associated miRNAs by miRNA antagonists or mimics [129,130]. Recent studies have shown powerful therapeutic effects of miRNAs in several disease models. For example, a miR-122 inhibitor showed efficacy *in vivo* in suppressing Hepatitis C virus infection in primates [131].

MiRNA antagonists are typically chemically modified single-stranded oligonucleotides with complementary sequences to the miRNAs of interest, which competitively bind to the endogenous miRNAs. The commonly used chemical modifications include cholesterol-conjugated 2'-O-methyl modification (antagomiRs) and locked-nucleic acid modification (LNA) [131,132]. MiRNA "sponges" contain

complementary binding sites for the miRNAs of interest and have the advantage of blocking a whole family of related miRNAs or achieving cell-type specific miRNA silencing [133]. MiRNA mimics can be chemically modified double-stranded miRNAs or miRNAs expressed by viral vectors, including retrovirus, lentivirus and adeno-associated virus.

MiRNA-based therapeutics is still in the early stages, however, inhibition of some miRNAs has been promising for the future treatment of cardiovascular diseases, such as miR-92a [134] and the miR-15 family [135]. To date, there is only one antagomiR in clinical trials; Miravirsen, an inhibitor of miR-122, against the Hepatitis C virus (HCV). Just recently, data from the phase 2a trial were released indicating that Miravirsen provided continuous and prolonged antiviral activity and was well tolerated in patients infected with HCV.

These promising clinical outcomes promote the research for additional miRNA therapeutic targets and new techniques for efficient *in vivo* delivery.

Chapter II - Aim of the Study

Aim of the study

Gestational diabetes mellitus (GDM) is a pregnancy-specific condition concerning approximately 7% of all pregnancies and is associated with long term adverse outcomes for the offspring. GDM leads to fetal hyperglycemia and endothelial dysfunction in the fetal circulation which might be responsible for the increased incidence of type 2 diabetes (T2D) and cardiovascular risk observed later in life in the offspring [2–4].

Molecular mechanisms involved in GDM-elicited outcomes are still unclear, however epigenetic regulation and microRNAs (miRNAs) are likely to play a role. Epigenetic mechanisms induce long-term gene expression changes in response to *in utero* environmental perturbations [32]. Moreover, miRNAs control the function of endothelial cells (ECs) under physiological and pathological conditions and can target the epigenetic machinery [99,101].

The aim of this study was to investigate the functional and expressional impact of GDM on human umbilical vein endothelial cells (HUVECs) focusing on the role of miR-101 and its target the Enhancer of Zeste Homologue-2 (EZH2). To this end, we isolated HUVECs from the umbilical cords of GDM and control healthy pregnancies. These cells represent an expedient *in vitro* model allowing for non-invasive analyses of the effect of the uterine environment on the fetal endothelium.

The first objective was to investigate the impact of GDM on the functional capabilities of HUVECs, with particular emphasis on apoptosis, migration, proliferation and tube formation. Secondly, we evaluated the expression of EZH2 (both EZH2 α and β isoforms) and miR101 to see whether they may affect endothelial function in diabetic conditions.

Chapter III – Materials and Methods

3.1 Study subjects and ethics

Umbilical cords were collected upon delivery from 24 full-term healthy and 22 full-term gestational diabetic pregnancies. The characteristics of the donors are presented in Table IV.

The study conforms to the principles outlined in the Declaration of Helsinki. Approval was granted by the ethics committee of the Faculty of Medicine, University of Sassari, and all mothers were fully informed and provided consent. Patients at 24-28 weeks gestation with basal glycemia >95 mg/dL (i.e. following an overnight fast) and >155 mg/dL two hours after a 75 gram oral glucose load were diagnosed as having gestational diabetes mellitus (GDM).

Human umbilical vein endothelial cells (HUVECs) were isolated at the University of Sassari, Italy, and exported to the University of Bristol, UK, where all experiments were performed. Import, storage and use of HUVECs samples in Bristol for this study were approved by NRES Committee West Midlands (REC reference: 12/WM/0366; IRAS Project Code: 113869).

3.2 Isolation and culture of Human Umbilical Vein Endothelial cells (HUVECs)

HUVECs were isolated from the umbilical cord vein of the newborn as described previously [136,137].

The two ends of the cord were cut with a sterile scalpel and a cannula was introduced at one end of the vein, which was the widest vessel having a thick lumen as shown in Figure 3.1. The vein was washed twice using a 30 ml syringe with 30 ml phosphate-buffered saline (PBS) so that the cord was clean and there was no blood or clot visible. HUVECs were flushed out after digestion for 10 mins at 37°C with 0.05% (w/v) type II collagenase from *Clostridium histolyticum* (Sigma-Aldrich, UK), prepared in medium M199 (Life Technologies, UK) supplemented with 100 U/ml of penicillin G sodium salt and 100 µg/ml streptomycin (Life Technologies, UK). The cellular suspensions were then collected and centrifuged at 1000×g for 10 minutes. The supernatant was carefully discarded and the pellet was resuspended in 5 ml of M199 medium supplemented with 10% (v/v) fetal calf serum (FCS), 10% (v/v) newborn-calf serum (NBCS) (Life Technologies, UK), 2mM glutamine and 1% penicillin/streptomycin.

The cells were then plated in 25 cm^2 tissue culture flasks (Corning, US) pre-treated with 0.1 % gelatin (Sigma-Aldrich, UK) and cultured in 5% CO_2 in a 37°C humidity incubator. The medium was changed every two days. After one week culture, the adherent cells were harvested with 0.05% trypsin-EDTA (Life Technologies, UK) treatment and sub-cultured. From passage 2, HUVECs were cultured in endothelial cell basal medium EGM-2 (Lonza, UK), following the addition of a SingleQuots™ Kit (Lonza, UK) and additional 8% FBS (10% FBS in total).

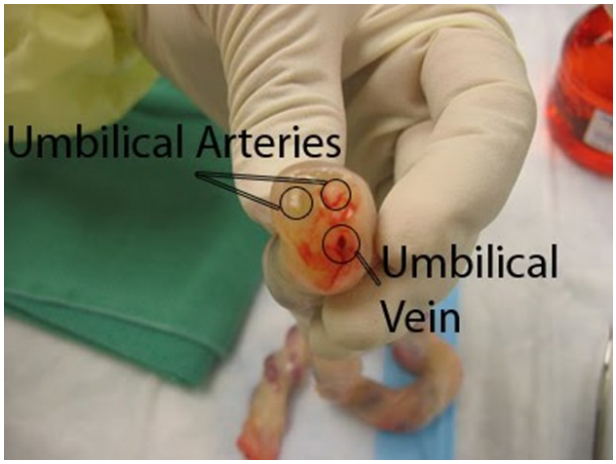


Figure 3.1 Human umbilical vein and arteries
The picture indicates the location of the umbilical artery and umbilical vein. The HUVECs are isolated from the umbilical vein. The image is adapted from http://www.slhd.nsw.gov.au

3.3 Immunocytochemistry

Isolated HUVECs were characterized by immunocytochemistry. HUVECs were seeded in round glass microscope slides on a 24 multiwell plate at a density of $4x10^4$ cells/well in EGM-2 10% FBS. The cells were then rinsed in PBS and fixed in 4% PFA for 20 minutes at room temperature. Cells were permeabilised with 0.1% Triton X-100 (Sigma Aldrich, UK) in PBS and then blocked in 0.5% goat serum (Vector Laboratories, UK) in PBS for one hour at room temperature. Primary antibodies for human CD-31/PECAM‑1 (R&D Systems, UK, 1:50), CD-144/VE-Cadherin (Santa Cruz Biotechnology, UK 1:50), Von Willebrand Factor (Dako, UK, 1:50) were added in 1% goat serum and incubated overnight at 4°C. The cells were washed in PBS three times

before being incubated for 1 hour in the dark with anti-mouse secondary antibody, 1:400 (Invitrogen).

Finally, the nuclei were counterstained with DAPI 1:1000 (Invitrogen, UK) for 4 minutes in the dark. After a final wash in PBS, the slides were mounted using a mounting medium for fluorescence (Southern Biotech, UK), and cell images were captured using an Olympus BX40 microscope, an in-line digital camera and the Image-Pro Plus (Media Cybernetics, UK) software. HUVECs were used from passages 2 to 6 to ensure their endothelial characteristics.

3.4 Experiments concerning the exposure of cells to high glucose

The experimental medium containing a high concentration of glucose was prepared directly before the experiments by solubilizing the appropriate amount of powdered D-glucose or L-glucose (Sigma-Aldrich, UK) in EGM-2, with subsequent filtration and supplementation with 10% FBS and 1% penicillin/streptomycin. The final concentrations of glucose in the two media were 12.5 mM and 25 mM.

HUVECs obtained from the umbilical vein of healthy donors were cultured for 48 hours with the two glucose concentrations (12.5 mM and 25 mM) to mimic hyperglycemic conditions. L-glucose was used as an osmotic control for each concentration of D-glucose.

3.5 MiRNA and siRNA transient HUVECs transfection

To alter miR-101 and Enhancer of Zeste Homologue 2 (EZH2) levels in GDM-HUVEC, the cells were seeded on a 6-well plate at a density of $2x10^5$ cells per well in 2 mL complete EGM-2 medium and grown for 24 hours until 70–80% confluent. The cells were then maintained in OptiMEM serum-free medium (Life Technologies, UK) for 2 hours prior transfection and then transfected with 12.5 nM of pre-miR-101 (Thermo Fisher Scientific, Assay ID: MC11414) anti-miR-101, (Thermo Fisher Scientific, Assay ID: MH11414, UK), miRNA scrambled controls (Thermo Fisher Scientific, UK), EZH2 siRNA (Qiagen, Cat no. SI02665166, UK) or siRNA negative control (Qiagen, UK).

The siRNA and miRNA molecules were reconstituted to their final concentration by addition of RNAase-free water and stored at -20°C. The final concentration of the oligomers was 5 μM for pre-and anti-miR-101, 50 μM for miRNA scrambled control and 20 μM for EZH2 siRNA and siRNA negative control. Oligonucleotides were transfected into HUVECs using Lipofectamine 2000 (Life Technologies, UK).

Briefly, in sterile tubes was prepared the Mix A containing 100 μl of serum-free OptiMEM and 2 μl of Lipofectamine 2000, which was incubated for 15 minutes at room temperature. Then the Mix B was prepared containing 100 μl of serum-free OptiMEM and the oligomers. Mix A and B were then combined by mixing gently and incubated for 15 minutes at room temperature. Next, 100 μl of DNA-liposomes complexes were added to each well mixing gently and the cells were incubated at 37°C and 5% CO_2 for 5 hours. After 5 hours, the transfection medium was replaced by EGM-2 (10% FBS) and after 48 hours the cells were harvested and RNA and protein expression was analyzed by q-PCR and Western blot, respectively. The above mentioned protocol has been scaled down to accommodate different cell numbers.

3.6 HUVECs adenoviral transduction experiments

The recombinant adenoviruses carrying human *EZH2-alpha*, human *EZH2-beta* or an empty vector (Null) were kindly provided by Professor Urrutia (Laboratory of Epigenetics and Chromatin Dynamics, Mayo Clinic, Rochester, MN, 55905, USA) and have been extensively described [9].

For the adenoviral transduction, HUVECs were seeded on a 12-well plate at a density of $1x10^5$ cells per well in 1 mL complete EGM-2 medium and grown for 24 hours until 70–80% confluent. Cells were then infected overnight with adenoviruses (Ad) at 150 multiplicity of infection (MOI) in EGM-2 (10% FBS). The cells were harvested after 48 hours and EZH2 RNA and protein expression was analyzed by q-PCR and Western blot, respectively.

3.7 Apoptosis assay

Apoptosis was assessed using the Cell Death Detection ELISA colorimetric kit (Roche Life Scientific, UK) which specifically detects histone-associated DNA fragments. During apoptosis, endonucleases cleave the double stranded DNA at

internucleosomal regions generating mono- and oligonucleosomes. The DNA fragments thus formed are enriched in the cytoplasm of apoptotic cells and can be measured.

The experiment was performed as per the manufacturer's instructions. HUVECs were cultured on 6-well plates at a density of $2x10^5$ cells per well and grown until 90% confluent. The cells where then collected and centrifuged at 400 x g for 5 minutes. The supernatant was carefully removed, and the cell pellet was resuspended and incubated in lysis buffer for 30 minutes at room temperature. The lysate was then centrifuged at 13000 x g for 10 minutes and 20 µl of the lysate was transferred to the anti-histone antibody coated microplate and was incubated for 90 minutes. The anti-DNA-POD conjugate solution was then added to each well and incubated under gentle shaking (300 rpm) for 90 minutes at room temperature The solution was removed by up-turning the plate and the substrate solution was added to the wells and incubated for 15 minutes. The absorbance was measured at 405 nm with an ELISA plate reader (Opsys MR, Dynex Technologies US) and the obtained values were reported as a fold change (*vs.* controls).

3.8 BrdU proliferation assay

The BrdU assay works on the principle that 5-Bromo-2'deoxy-Uridine (BrdU) is incorporated into freshly synthesized DNA. Cells are then fixed and the DNA is partially digested which allows the binding of peroxidase-labelled anti-BrdU antibodies. Finally peroxidase substrate is added, which is cleaved by the peroxidase enzyme generating a chromogenic product. Absorbance is proportional to the amount of BrdU incorporated into cellular DNA.

The BrdU assay was performed by using Cell Proliferation ELISA BrdU colorimetric kit (Roche Life Sciences, UK) following the manufacturer's protocol. Briefly, the HUVECs were seeded in 96-well plates at a density of $2x10^3$ cells per well and grown for 24 hours until 70–80% confluent. Then then the cells were incubated for 1 hour in EGM-2 without FBS and cultured for 24 hours with 0.5% or 10% FBS, in the presence of BrdU at a final concentration of 10 µM. After the 24 hours incubation the supernatant was removed by up-turning the plate. The DNA in the cells was denatured by incubation with FixDenat solution for 30 minutes at room temperature. FixDenat was then removed and anti-BrdU-POD was added for 90 minutes. The cells were then

washed with the washing buffer and incubated with substrate solution for 10 minutes at room temperature until the color development was sufficient for photometric detection.

The plates were read with an ELISA plate reader (Opsys MR, Dynex Technologies US) at 340 nm with the reference wavelength set at 370 nm. The ratio between the average proliferative capacity of 0.5% FBS and 10% FBS cultures gave an indication of FBS-stimulated proliferation.

3.9 *In vitro* scratch assay

The *in vitro* scratch assay is a method to study cell migration. Cells were seeded in a 12-well plate ($1x10^5$ cells/well) and grown until confluence in EGM-2 10% FBS. Once a confluent monolayer of cells had formed, the cell monolayer was scratched in a straight line with a sterile P200 pipette tip to create a gap in the center of the well. After scratching, the medium was aspirated and discarded, and the cells were washed with medium to remove debris and to smooth the edge of the scratch. After washing, fresh medium supplemented with 2 mM hydroxyurea (Sigma-Aldrich, UK) was added to arrest cell growth and the plate was incubated at 37°C and 5% CO_2.

Images were taken at 0, 6 and 10 hours at 5X magnification using a bright field inverted microscope (Carl Zeiss, UK). Image J (NIH) was used to calculate the wound area at the three time points. The final result obtained was the average speed of closure of the wound (in mm^2/h).

3.10 Tube formation assay on Matrigel

The tube-formation assay is a well-established *in vitro* angiogenesis assay based on the ability of endothelial cells (ECs) to form three-dimensional capillary-like tubular structures, when cultured on a gel of growth factor-reduced basement membrane extracts. During the assay, endothelial cells differentiate and directionally migrate to form the tubular polygonal networks of blood vessels.

Growth Factor Reduced Matrigel (Corning, UK) was thawed overnight at 4°C and kept on ice before being added to 96 well plates; 40 µL of Matrigel were then distributed to each well and allowed to solidify at 37°C for 30 minutes. HUVECs were

placed on Matrigel in triplicate, at a density of $1.5X10^4$ cells/well in 100 µL of complete EGM-2, and incubated for 24 hours at 37°C in a humidified atmosphere with 5% CO^2.

Images were taken after 6 and 24 hours at 5X magnification using a bright field inverted microscope. Image J was used to calculate the total tube length (mm) as a parameter of angiogenic capacity *in vitro*.

3.11 Total RNA isolation for mRNA and miRNA analysis

RNA was isolated from cultured cells using the miRNeasy Mini kit (Qiagen, UK) which enables purification of total RNA, including small RNAs from approximately 18 nucleotides, such as miRNAs.

RNA was eluted with 35 µl of RNAase-free water. The concentration of RNA was determined by Nanodrop (Thermo Scientific, UK) and A260/A280 ratios were also calculated for each sample to assess the purity of RNA. Samples with ratios smaller than 1.7 or greater than 2.1 were discarded.

3.12 Quantitative Reverse Transcription Polymerase Chain Reaction (qRT-PCR) for mRNA

The qRT-PCR is a combination of two steps including reverse transcription and quantitative polymerase chain reaction. In the first step, an input of 300 ng of total RNA was reverse transcribed using QuantiTect Reverse Transcription kit (Qiagen, UK) according to the manufacturer's protocol. RNA was reverse transcribed into cDNA using random hexamer primers. The cDNA was then distributed to the appropriate wells of a 96 well plates with gene-specific primers for EZH2 (Sigma), EZH2 total, EZH2-α or EZH2-β [9] and Power SYBR Green qPCR Master Mix (Life Technologies, UK), and quantified using the LightCycler480 qPCR detection system (Roche Life Sciences, UK).

Levels of mRNA were normalized to β-actin, selected as the reference gene. Relative levels of mRNAs were calculated from threshold cycle (Ct) values using the 2^(-ΔΔCt) method. Using this method, we obtained the fold changes in gene expression normalized to an internal reference gene [138]. The primer sequences used are presented in Table II.

Genes	Forward	Reverse
Beta-actin	TGGACATCCGCAAAGACCTGTA	GGGCAGTGATCTCCTTCTGCAT
EZH2	CCTGAAGTATGTCGGCATCGAAAGAG-	TGCAAAAATTCACTGGTACAAAACACT
EZH2 total	CGAGCTCCTCTGAAGCAAAT	AACCTAGCAATGGCACAGAAA
EZH2 alpha	GCGGGACTAGGGAGTGTTC	AAAACAGTTTCATCTTCCACCA
EZH2 beta	GGGACTAGGGAGGTGGAAGA	GCATTCACCAACTCCACAAA

Table II: Details of primer sequences used for this study.

3.13 Quantitative Reverse Transcription Polymerase Chain Reaction (qRT-PCR) for microRNA

For miRNA analyses, reverse transcription was performed using the TaqMan MicroRNA Reverse Transcription kit (Life Technologies, UK). All reverse transcription reactions were performed in accordance with the manufacturers' protocols using an input of 10 ng RNA for each reaction. Real-time PCR was performed using the TaqMan universal master mix with the LightCycler480 qPCR detection system (Roche Life Science, UK). Individual microRNA primers for both RT and qPCR were included with TaqMan MicroRNA assay sets (Life Technologies, UK). U6 snRNA (Thermo Fisher Scientific, Assay ID: 001973) was used as endogenous control for normalization. Relative levels of mRNAs and miRNAs were calculated from the threshold cycle (Ct) values using the 2^(-ΔΔCt) method [138].

3.14 Western blot experiments

Cell nuclear extracts were prepared using a previously published protocol [139]. Briefly, cells were washed twice with cold PBS then resuspended in buffer A (10mM Hepes pH 7.5, 10mM KCl, 1.5mM MgCl2, 0.34M Sucrose, 10% Glycerol, 0.1% TritonX-100) supplemented with protease inhibitors (1mM DTT, 0.5mM PMSF, 2 µl/ml Protease Inhibitors Cocktails, Sigma-Aldrich,. UK) and incubated at 4°C on a rotator for 30 minutes to improve lysis. Nuclei were isolated by centrifugation at 6500×g for 5

minutes at 4 °C, washed once with buffer A (depleted of Triton X-100) and subsequently resuspended in buffer B (3 mM EDTA, 0.2 mM EGTA, plus protease inhibitors).

Nuclear protein fractions extracted from HUVECs were electrophoresed through 10% Bis-Tris gel and transferred to PVDF membranes, 0.2 µm pores, (GE Life Sciences, UK) by the Bio-Rad wet transfer system. Blots were blocked for 2 hours in 5% BSA solubilized in TBS-Tween then probed overnight with antibodies against EZH2 (Active Motif, 1:2000); EZH2 total (1:500), EZH2-alpha (1:500), EZH2-beta (1:500) [9], anti-trimethyl-Histone H3 (Lys27) (UPSTATE Cell Signaling, US, 1:2000); anti-Histone H3 (Active Motif, UK, 1:2000); anti-Lamin A/C (Active Motif, UK 1:1000). After three washes (TBS + 0.05% Tween 20) blots were stained with HRP-conjugated secondary antibodies (Santa Cruz Biotechnology). Bands were visualized using the ECL prime system and photographic film (GE Life Sciences, UK) and quantified using Image J (NIH).

3.15 Chromatin immunoprecipitation (ChIP)

ChIP assays were performed in order to study EZH2 binding to the miR-101 promoter in both GDM-HUVECs and healthy HUVECs or in healthy HUVECs exposed to high concentrations of D-glucose (25 mM). Cells were fixed in 1% formaldehyde/PBS to cross-link proteins to DNA. After 10 minutes of incubation at RT, the cross-linking has been stopped by adding glycine to a final concentration of 0.125 M. The cells were then washed three times in PBS and lysed in SDS buffer (100 mM NaCl, 50 mM Tris-HCl (pH 8), 5 mM EDTA (pH 8), 0.2% NaN3, SDS 0.5%). The chromatin pellet has been obtained by centrifuging 6 min at 1200 rpm at 4°C. The only supernatant was kept and resuspended to the final volume of 300 µl with ice-cold IP Buffer (1 vol of SDS Buffer : 0.5 vol Triton Dilution Buffer). Triton dilution buffer was made with 100 mM Tris-HCl (pH 8.6), 100 mM NaCl, 5 mM EDTA (pH 8), 0.2% NaN3, 5% Triton-X100.

The chromatin was sonicated (3x9 cycles 30”ON/30”OFF) to an average DNA length of 400–500bp using a Bioruptor sonicator (Diagenode, Belgium). Immunoprecipitation was performed in 1 ml volume with the addition of 3-5 µg of the EZH2 antibody (Active Motif, UK), H3K27me3 antibody (Merck Millipore, UK) and control IgGs (Merck Millipore, UK). The following day, immune complexes were

collected with purified protein A-magnetic beads (Life Technologies, UK) for 3 hours at 4 °C with rotation, washed and DNA eluted by reverse crosslinking at 65 °C for 4 hours.

Aliquots of immunoprecipitated DNA were analyzed in triplicate by real-time quantitative PCR analysis with Power SYBR Green qPCR Master Mix (Life Technologies, UK) and primers specific for the putative regulatory region of *miR-101* gene (UCSC Genome Browser, Table III) bound by EZH2 and H3K27me3 within the *miR-101* transcription start site (Chr1: 65532194). ChIP-enriched DNA on the target genomic regions was assessed relative to the input DNA and IgG control.

miR-101 promoter region (distance from TSS)	Forward	Reverse
-705/-682 bp	CTTCTTTCTTCCTGGGTACG	TCCTTCACTTCATGGGGAG
-562/-476	AATAACTCTCCCTATGCCCC	GCCATCTTACCTTCCATCAG
-396/+3	TCAGCTCACCTCTCCTTCAA	GAGGGGTGCTTTGCTGTAAT

Table III: PCR primers used for amplification of miR-101 promoter regions.

3.16 Molecular cloning of mir-101 promoter and activity assessment by luciferase reporter assay

The putative regulatory element of the mir-101 promoter was cloned by PCR (KOD polymerase, MERCK Millipore, UK) from human genomic DNA. A larger fragment was initially cloned using primers (forward 5'-CTCGGTTTCTCTGCACGTTCG-3' and reverse 5'-GGATTATAAAGCTAGGAGGCT-3') and a second nested PCR was performed to add clamp and restriction endonuclease NheI and BglII (NEBiolabs, UK) recognition sites respectively using GCACGCTAGCCTCGGTTTCTCTGCACGTTCG and GCACAGATCTGACAGCAGATTCCATTAG. The second fragment including nucleotides 65532188 to 65531494 (Homo Sapiens Chromosome1, GRCh37.p13

primary assembly) was cloned upstream (NHE1-BglII sites) of the SV40 promoter of the pGL3-Promoter Luciferase Reporter Vector (Promega Corporation, UK).

For constructs transfection HUVECs were seeded in 24-well plates at a density of $6x10^4$ cells per well in 0.5 mL complete EGM-2 medium and grown for 24 hours. Cells were then co-transfected with 0.075 µg renilla (pRLTK, internal control (Promega Corporation, UK), 0.75 µg pGL3 (control vector) or 0.75 µg of pGL3 mir-101 promoter (all Promega Corporation, UK), along with 200 µl OptiMEM. Luciferase reporter vectors were transfected by using Lipofectamine 2000 (Life Technologies, UK) for 5 hours in OptiMem. Cells were then transduced with adenovirus overnight. Three days after transfection, cells were harvested and assayed with the Dual-Luciferase Assay system (Promega Corporation, UK), according to the manufacturer's protocol.

The readings were performed using a Glomax 96 microplate luminometer (Promega, UK). Each treatment was performed in triplicate in three independent experiments. The results were expressed as relative luciferase activity.

3.17 Statistical analysis

Data are expressed as mean ± standard error of the mean (SEM) from at least three independent experiments. Data were assessed for normality using the Shapiro-Wilk test, and differences in two-group comparisons were tested using the unpaired or paired Student's *t*-test, where relevant (for parametric data) or the Mann-Whitney U test (for non-parametric data). Where there were three or more groups, a one-way ANOVA was performed with a Tukey *post-hoc* test. All statistical analyses were performed using GraphPad Prism for Windows v6.0 (GraphPad Software Inc.). *P* values < 0.05 were considered statistically significant.

Chapter IV - Results

4.1 HUVECs isolation and characterization

HUVECs collected from the umbilical cords of newborns delivered by gestational diabetes mellitus (GDM) mothers. GDM-HUVECs have been considered an expedient *in vitro* model to study the molecular consequences of long term, chronic hyperglycemia [67,140]

Therefore, in order to perform our experiments, we first isolated HUVECs from the umbilical cord vein of both healthy and GDM-complicated pregnancies. The characteristics of the donors are presented below in Table IV.

	Healthy n=24	Gestational diabetes n=22
Age (years)	31.12 ± 6.54	35.13 ± 7.41
Smokers (n)	1	1
Weight (Kg)	77.00 ± 15.48	73.73 ± 14.74
Obese (n)	3	4
Hypertensive (n)	1	1
Epidural delivery (n)	3	6
Pregnancy at risk (n)	0	1
Baby birth weight (Kg)	3.180 ± 0.43	3.45 ± 0.60

Table IV: Characteristics of the study subjects
No statistically significant differences were found between the two groups for any of the parameters reported above. Quantitative data are expressed as mean ± standard deviation (SD)

Isolated HUVECs were then characterized by immunocytochemical analysis for three reported endothelial cell (EC) markers [141,142]: Cluster of Differentiation 31 (CD-31), Cluster of differentiation 44 (CD-144) and Von Willebrand Factor (vWf). As shown in Figure 4.1, HUVECs were positive for CD-31 (A), CD-144 (B) and vWF (C) In negative controls, where the primary antibody had been omitted, no fluorescent signal was detected (D). These results confirmed the endothelial cell identity of HUVECs isolated with our protocol [136,137].

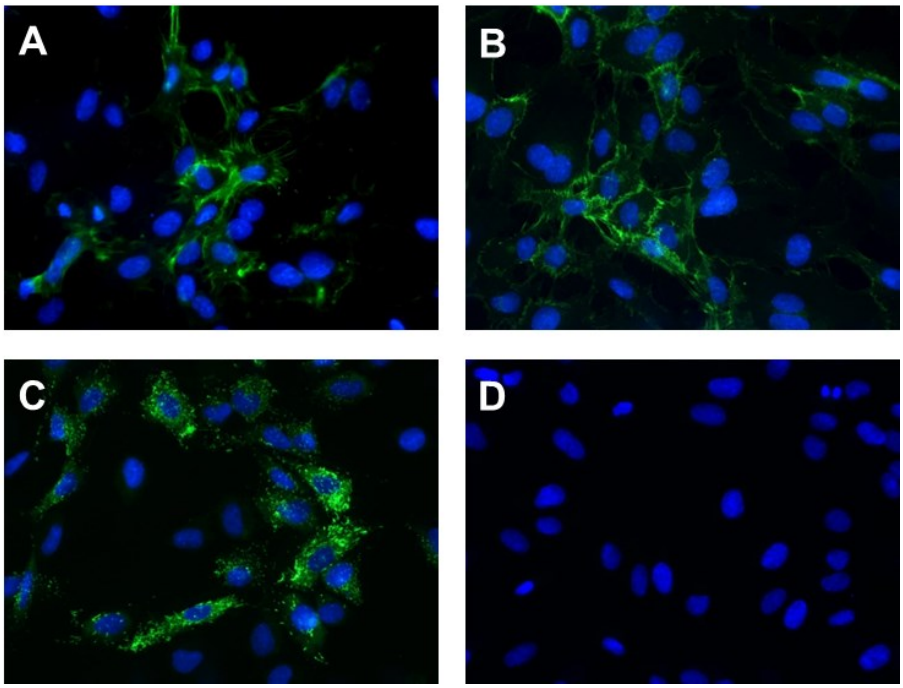


Figure 4.1: Immunofluorescence analysis of HUVECs
HUVECs were isolated from umbilical cords of both GDM and healthy control pregnancies and stained with primary antibodies against CD-31 **(A)**, CD-144 **(B)** or vWF **(C)**. Nuclei are stained with DAPI (blue). The images show that HUVECs are positive for the endothelial cell markers. Negative control HUVECs incubated only with the secondary antibody (green) demonstrate no false positives **(D)**. Images were captured at 40X magnification using an Olympus BX40 microscope, an in-line digital camera and the Image-Pro Plus software.

4.2 Gestational diabetes mellitus induces phenotypic alterations in HUVECs

In order to investigate potential modifications elicited by GDM in the HUVECs' phenotype, we cultured the cells (from both normal and GDM pregnancies) *in vitro* for several passages under physiological glucose conditions.

As expected GDM-HUVECs showed an increase in the relative apoptotic activity compared to healthy HUVECs controls (Figure 4.2 A) and a lower proliferative index after stimulation with fetal bovine serum (Figure 4.2 B). Moreover, GDM-HUVECs presented a reduced capacity to form cellular networks on Matrigel (Figure 4.2 C) and an impaired migration capability measured using a scratch assay (Figure 4.2 D).

Our results are consistent with the hypothesized mechanism where hyperglycemia leads to endothelial dysfunction thus promoting diabetic vascular complications. Moreover these GDM-induced phenotypic alterations were observed after 5 to 6

passages in GDM-HUVECs cultured under normal glucose conditions, which suggests that they likely mimic long-term effects of the GDM *in utero* environment.

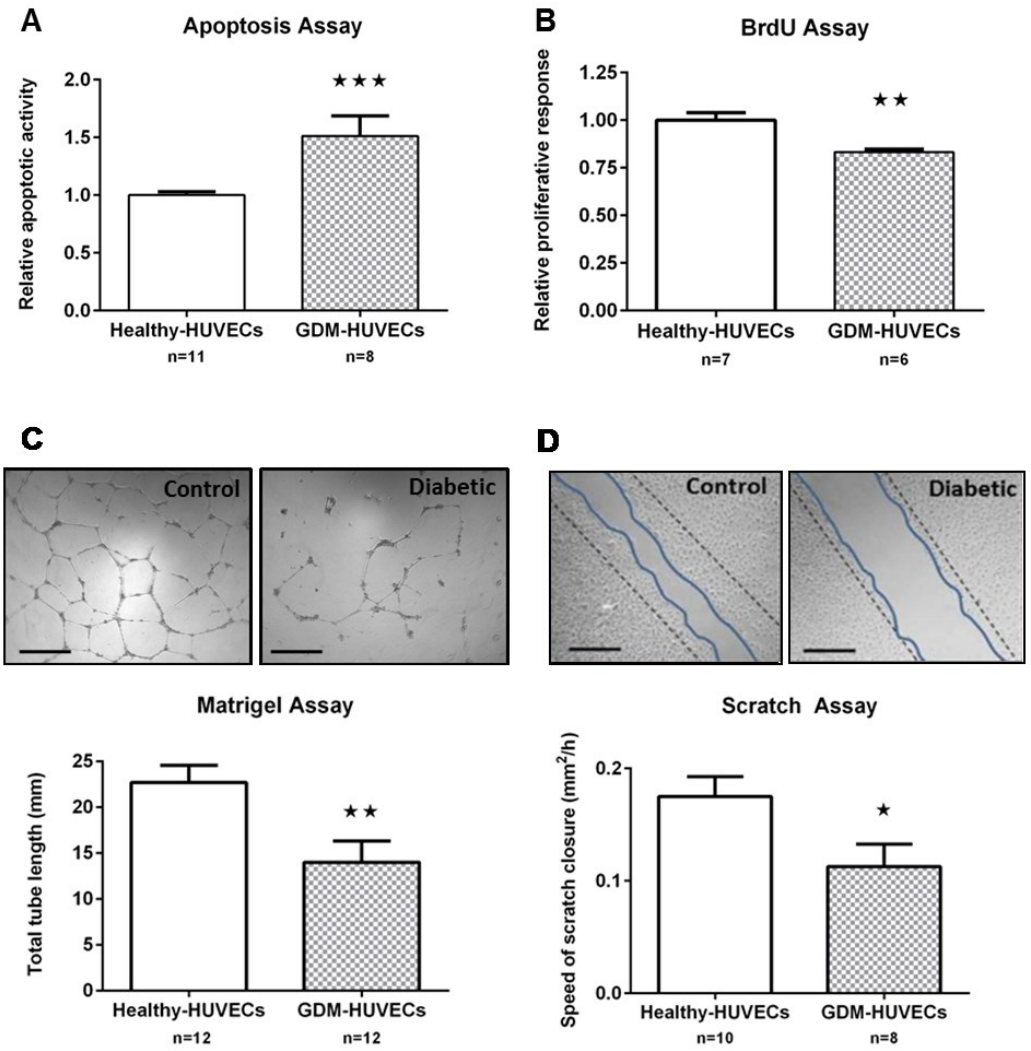


Figure 4.2: Phenotypic characterization of GDM-HUVECs
The graphs show that in comparison with Healthy-HUVECs, GDM-HUVECs presented an increased apoptosis rate (assessed using a Cell Death Detection ELISA and expressed as normalized absorbance units) **(A)** and an impaired capacity to proliferate (evaluated by BrdU incorporation assay and expressed as the ratio between the BrdU incorporation values in 0.5% and 10% FBS conditions) **(B)**. Moreover GDM-HUVECs showed an impaired capacity to form capillary-like structures on Matrigel **(C)** and to migrate and close a gap in a scratch assay (Scale bar 0.5 mm) **(D)**. All data are presented as mean ± standard error of the mean (SEM), **P*<0.05 ***P*<0.01, and ****P*<0.001 *vs.* healthy-HUVECs group. The number of donors used to prepare the tested HUVECs is reported on each graph.

4.3 MiR-101 is upregulated in HUVECs exposed to diabetic uterine environment

Besides classical gene regulation, miRNAs have emerged as post-transcriptional regulators of angiogenesis [99,100]. It has been recently shown that miR-101 upregulation exerted an anti-angiogenic effect on ECs under normal glucose conditions [12].

In order to explore the expressional levels of miR-101 in ECs exposed to hyperglycemia, we performed quantitative polymerase chain reaction (qPCR) analysis on GDM-HUVECs and healthy-HUVECs. We used the small nuclear RNA U6 (snRNAU6) as reference control, which was uniformly expressed in HUVECs in the presence or absence of the diabetic condition.

As showed in Figure 4.3, miR-101 expression was higher (≈ 3 fold increase ± 0.9169, $P<0.01$) in GDM-HUVECs when compared to healthy HUVECs, thus suggesting a potential involvement of miR-101 in the functional changes previously observed in GDM-HUVECs (Figure 4.1).

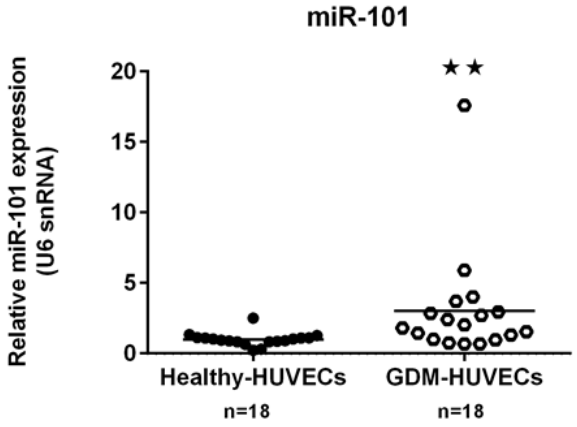


Figure 4.3: MiR 101 mRNA expression in GDM HUVECs
MiR-101 mRNA expression was assessed by qPCR in both GDM and healthy-HUVECs. The relative expression of miR-101 (normalized to snRNAU6) is higher in GDM-HUVECs when compared with that in healthy-HUVECs. Data are presented as mean ± SEM, $^{**}P<0.01$ *v.s* healthy-HUVECs group. The number of donors used to prepare the tested HUVECs is reported on the graph.

4.4 Effect of miR-101 dysregulation on GDM-HUVEC phenotype

To clarify the role of miR-101 on GDM-HUVEC phenotype, we first altered intracellular miR-101 levels by transfecting the cells with pre-miR-101 (to increase the miR-101 expression), anti-miR-101 (to decrease miR-101 expression) or a scramble sequence as a control (GDM-Scr). Figure 4.4 shows miR-101 expressional changes in response to successful transfection.

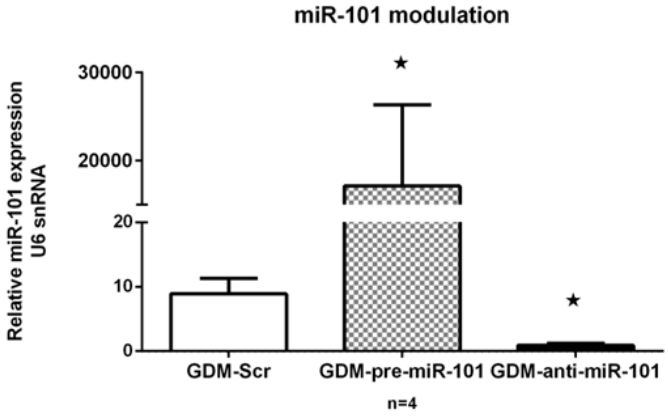


Figure 4.4: MiR-101 modulation in GDM-HUVECs
GDM-HUVECs were transfected with a precursor (GDM-pre-miR-101), inhibitor (GDM-anti-miR-101), or a scramble control (GDM-Scr) to modulate miR-101 levels. MiR-101 expression was tested by qPCR after 48 hours transfection. The graphs shows that miR-101 levels were effectively altered after transfection. Data are presented as mean ± SEM, **P*<0.05 *vs.* GDM-Scr group. The number of donors used to prepare the tested HUVECs is reported on the graph.

To understand whether miR-101 is responsible for GDM-HUVECs' impaired capabilities, we performed functional assays on GDM-HUVECs previously transfected with pre- miR-101 and anti-miR-101. We also used healthy HUVECs transfected with a scramble sequence (Healthy-Scr) as an additional control.

We found that anti-miR-101 had an anti-apoptotic effect on GDM-HUVECs (≈0.8 fold decrease ± 0.084 *vs.* GDM-Scr *P*<0.05), while a supplementary increase of miR-101 levels did not raise the apoptotic index (Figure 4.5 A). By contrast the proliferation capacity of GDM-HUVEC was unaffected by the forced miR-101 expressional changes (Figure 4.5 B).

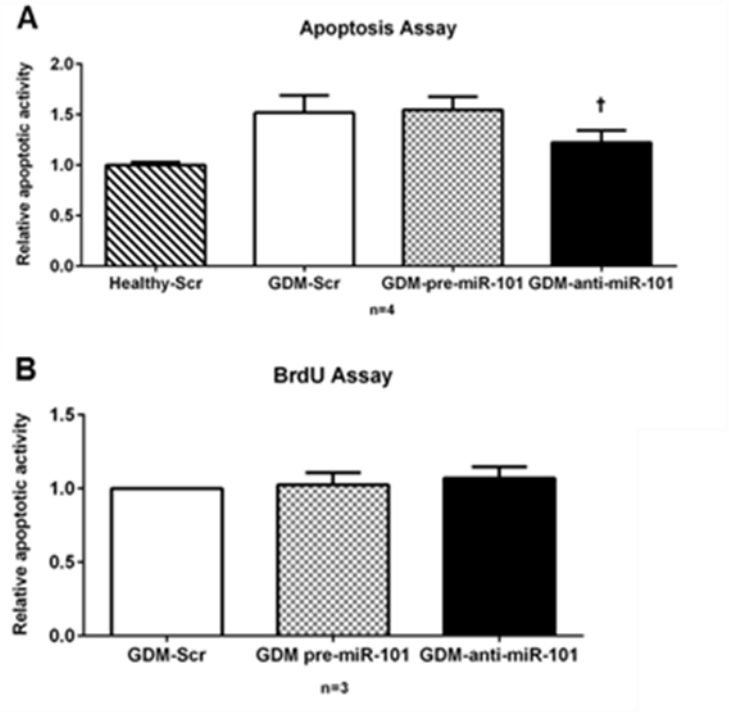


Figure 4.5: Effect of miR-101 modulation on GDM-HUVEC survival and proliferation
GDM-HUVECs were transfected with pre-miR-101 or anti-miR-101 using scrambled sequences as controls (Healthy-Scr. and GDM-Scr). Anti-miR-101 reduced the relative apoptotic activity in GDM-HUVECs **(A)**, but it did not affect cell proliferation **(B)**. All data are expressed as mean ± SEM. †P<0.05 *vs.* GDM-Scr. The number of donors used to prepare the tested HUVECs is reported in each panel.

Although an anti-angiogenic property of miR-101 on normal HUVECs has already been reported (Smits et al. 2011), its effect on GDM-HUVEC has not been investigated.

We observed that pre-miR-101 reduced the already compromised migratory capacity in GDM-HUVECs (0.060 ± 0.003 *vs.* 0.146 ± 0.016 mm^2/h, P<0.05), whereas anti-miR-101 did not exert any effect (0.104 ± 0.007 *vs.* 0.147 ± 0.016, Figure 4.6).

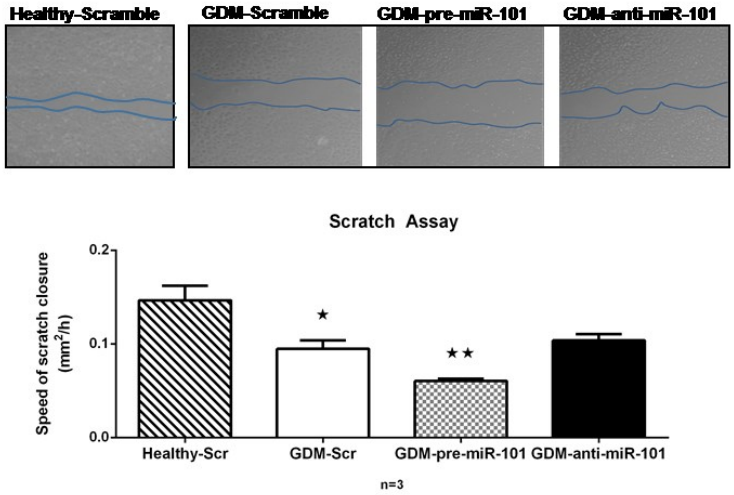


Figure 4.6: Effect of miR-101 modulation on GDM-HUVEC migration capabilities
GDM-HUVECs were transfected with pre-miR-101 or anti-miR-101 using scrambled sequences as controls (Healthy-Scr and GDM-Scr). The graph shows that pre-miR-101 reduced the migratory capacity (expressed in mm^2/h as the velocity of gap closure of the wounded area), whereas anti-miR-101 elicited no effect (scale bar 0.5 mm). All data are expressed as mean ± SEM. **P*<0.05 and ***P*<0.01 vs Healthy-Scr. The number of donors used to prepare the tested HUVECs is reported in each panel.

Moreover we found that miR-101 inhibition restored the GDM-HUVECs' angiogenic capacity measured as capillary like-tube formation on Matrigel (17.55 ± 0.991 *vs.* 11.63 ± 2.117 mm, *P*<0.05), while pre-miR-101 further decreased the capillary-like structures of GDM-HUVECs compared to GDM-Scr (4.741 ± 1.363 *vs.* 11.63 ± 2.117 mm, *P*<0.05*)* (Figure 4.7).

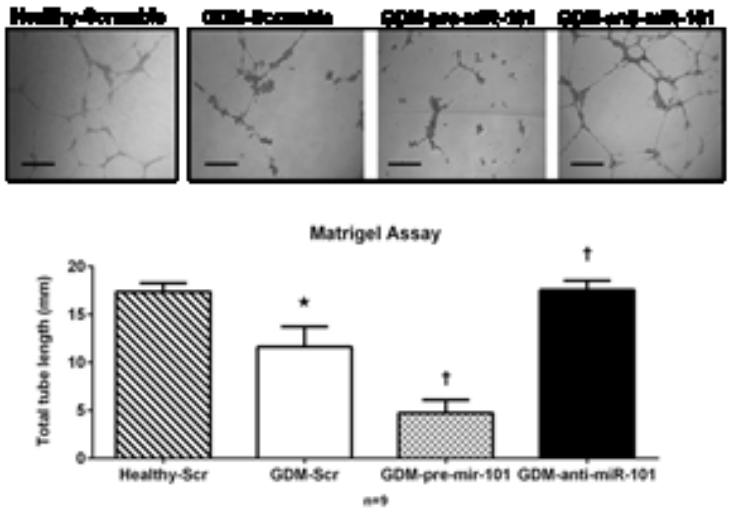


Figure 4.7: Effect of miR-101 modulation on GDM-HUVEC angiogenic capabilities
GDM-HUVECs were transfected with pre-miR-101 or anti-miR-101, using scrambled sequences as controls (Healthy-Scr. and GDM-Scr.). The angiogenic capacity of GDM-HUVECs (measured by network formation on Matrigel) was improved by anti-miR-101. Pre-mir-101 decreased the already compromised GDM-HUVECs' angiogenic capabilities. All data are expressed as mean ± SEM. **P*<0.05 and *vs*. Healthy-Scr; †*P*<0.05 *vs*. GDM-Scr. The number of donors used to prepare the tested HUVECs is reported in each panel.

From this experiments, we suggest that miR-101 upregulation in GDM-HUVECs is responsible of the impaired functional and angiogenic capacities presented by these cells.

4.5 Enhancer of Zeste Homologue 2 is downregulated in GDM-HUVECs

Previous studies have shown that Enhancer of Zest Homologue 2 (EZH2) is one of the targets of miR-101 and regulates angiogenesis [12,107,108]. Moreover, it has been recently demonstrated that the EZH2 locus generates, by alternative splicing, two major isoforms: EZH2α and EZH2β. Notably, the two different isoforms can each not only regulate distinct targets, but also share gene expression networks [9].As miR-101 is upregulated in GDM-HUVECs we had a look at EZH2 mRNA expression in these cells by qPCR. Consistently, the mRNA levels of EZH2 were reduced in GDM-HUVECs in comparison with healthy HUVECs (0.557 ± 0.067 *vs.* 1.736 ±0.442, *P*<0.05) (Figure 4.8 A). Interestingly, we noticed that the EZH2β isoform was decreased in GDM-HUVECs (0.860 ± 0.102 *vs.* 2.025 ± 0.513, *P*<0.05, Figure 4.8 B), whereas the EZH2α levels were unchanged, (1.167 ± 0.112 *vs*. 1.575 ± 0.245, Figure 4.8 C).

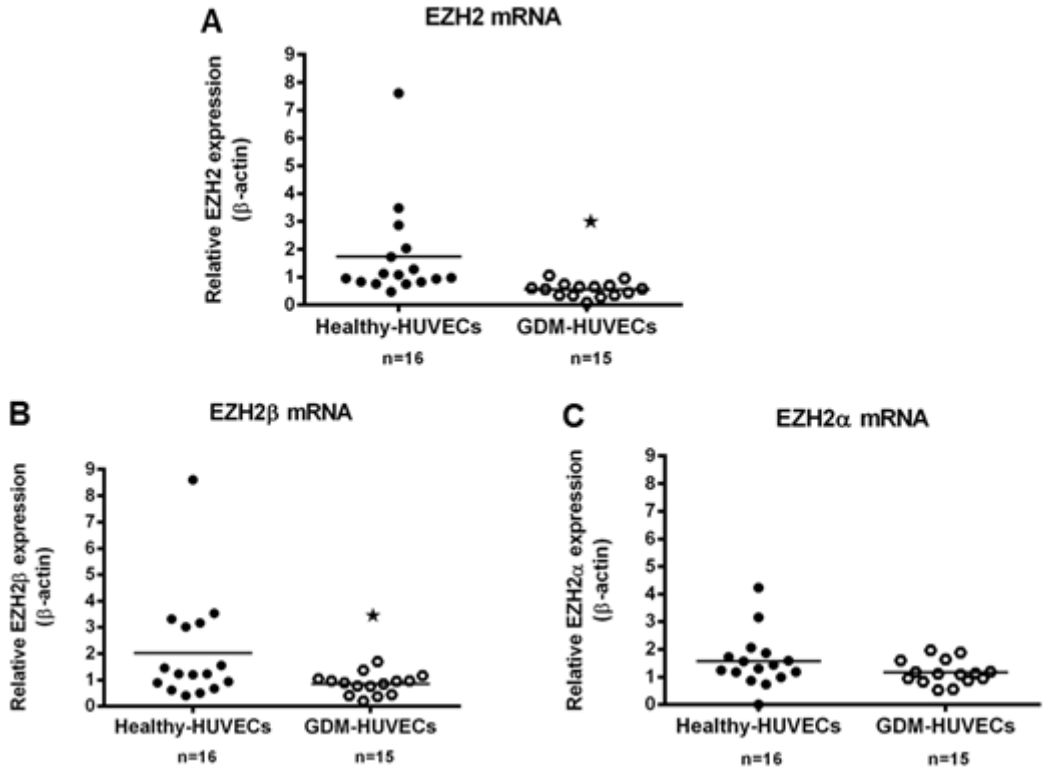


Figure 4.8: EZH2 mRNA expression in GDM-HUVECs
EZH2 mRNA expression was assessed by qPCR in both GDM and Healthy-HUVECs. The relative mRNA levels of EZH2 (normalized to β-actin) **(A)**, especially of EZH2β, were significantly reduced in GDM-HUVECs in comparison with Healthy-HUVECs **(B)**, whereas the relative expression of EZH2α was not **(C)**. All data are presented as mean ± SEM. **P*<0.05 *vs.* Healthy-HUVECs. The number of donors used to prepare the tested HUVECs is reported in each panel.

EZH2 protein levels were also reduced in GDM-HUVECs in comparison to healthy HUVECs as shown by Western blotting analysis (Figure 4.9 A). EZH2 proteins function as the key histone code writers of the trimethylation of histone H3 on lysine 27 (H3K27m3) that leads to long-term epigenetic gene silencing [112]. Accordingly we found that the levels of H3K27m3 protein were also decreased in GDM HUVECs compared to healthy HUVECs. (Figure 4.9 B).

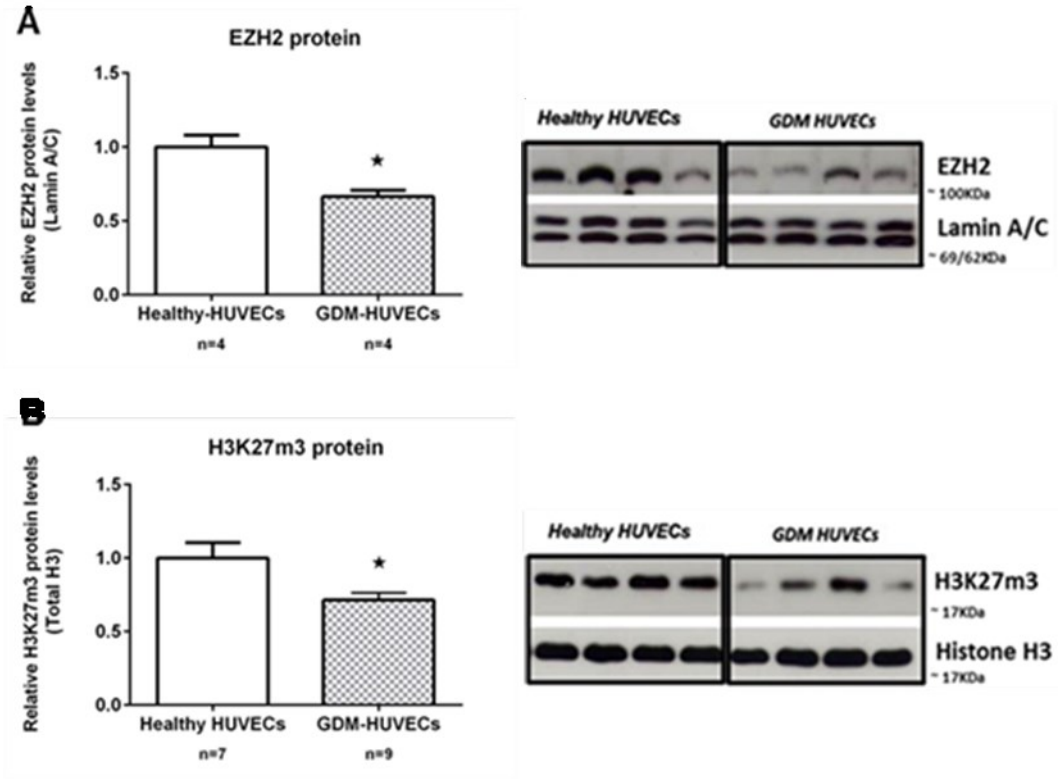


Figure 4.9: EZH2 and H3K27m3 proteins levels in GDM-HUVECs
Protein levels were determined by Western blotting analysis in GDM and Healthy-HUVECs. The graphs show that EZH2 was decreased in GDM-HUVECs compared to Healthy-HUVECs (normalized to lamin A/C) **(A)**. Accordingly, the H3K27m3, derived by EZH2 enzymatic activity, was also decreased (normalized to total H3) **(B)**. Data are presented as mean ± SEM. **P*<0.05 *vs*. Healthy-HUVECs. The number of donors used to prepare the tested HUVECs is reported in each panel.

To clarify the enzymatic activity of EZH2 isoforms on H3K27m3 in GDM-HUVECs, we separately overexpressed each isoform by using adenovirus-based (Ad.) transductions. An adenovirus carrying an empty vector (Ad.Null) was used as control. Figure 4.10 A shows increased mRNA levels of EZH2α (≈ 238 fold increase ± 43.98, *P*<0.001), and EZH2β (≈ 323 fold increase ± 63.72, *P*<0.001) after gene transfer. We observed that in GDM-HUVECs, Ad.EZH2β increased the H3K27m3 levels (≈ 2 fold increase ± 0.345, *P*<0.05 in comparison with Ad.Null), whereas Ad.EZH2α had no impact (Figure 4.10 B). From this experiment we concluded that in GDM-HUVECs only EZH2β may be involved in H3K27m3-mediated gene silencing.

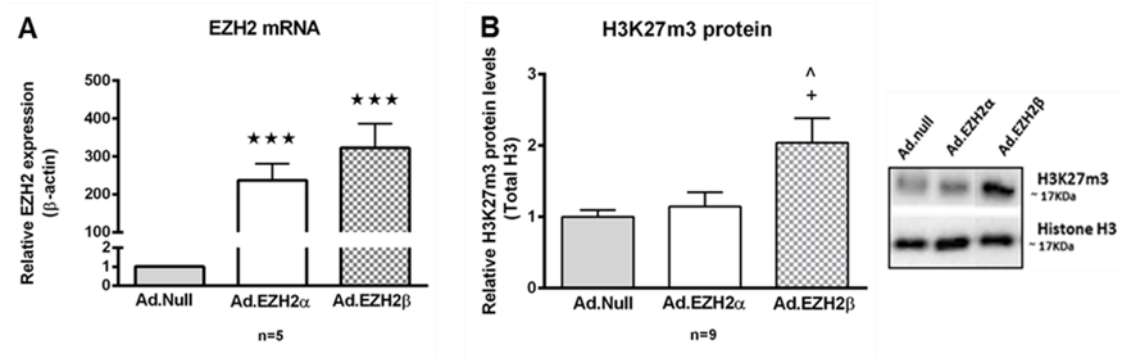


Figure 4.10: Adenovirus-mediated overexpression of EZH2α and EZH2β in GDM HUVECs. EZH2α and EZH2β overexpression was induced by adenovirus (Ad.) transduction. The relative expression of both EZH2 isoforms (normalized to β-actin) assessed by qPCR was successfully increased **(A)**. Ad. EZH2β overexpression increased H3K27me3 levels in GDM-HUVECs, whereas Ad.EZH2α was ineffective as shown by Western blot analysis **(B)**. All data are presented as mean ± SEM. ***P<0.001 *vs.* Healthy-HUVECs; +P<0.05 *vs.* Ad.Null; and $^{\wedge}P$<0.05 *vs.* Ad.EZH2α. The number of donors used to prepare the tested HUVECs is reported in each panel.

4.6 MiR-101 downregulates EZH2 expression in GDM-HUVECs

To confirm that miR-101 directly targets EZH2 for inhibition in GDM-HUVECs, we altered miR-101 levels by transfecting GDM-HUVECs with pre-miR-101 or anti-miR-101 using a scramble sequence as a control (GDM-Scr).

We first found that both pre-miR-101 and anti-miR-101 affected EZH2 mRNA expression (Figure 4.11 A). When looking specifically at the effect of miR-101 inhibition on each of the two EZH2 isoforms, we found that mRNA levels of both were increased compared to GDM-Scr (Figure 4.11 B).

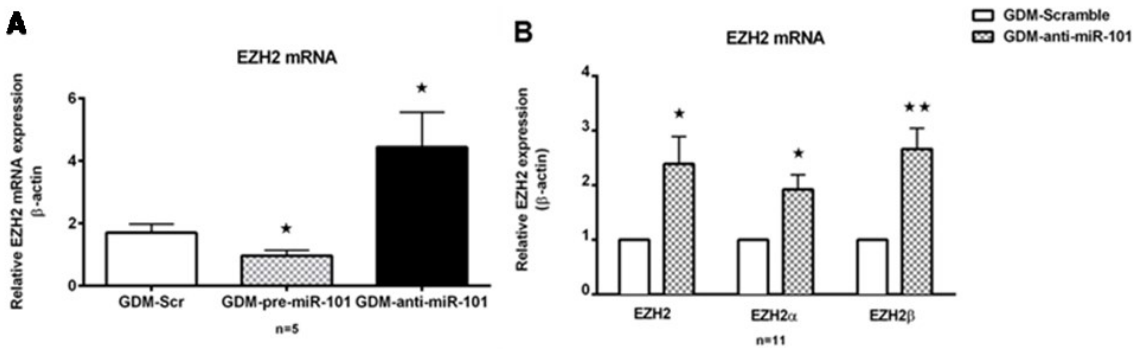


Figure 4.11: MiR-101 regulates EZH2 mRNA levels in GDM-HUVECs
GDM-HUVECs were transfected with pre-miR-101, anti-miR-101 or a scramble sequence (GDM-Scr) to modulate miR-101 expression levels. Relative expression of EZH2 mRNA (normalized to β-actin) was reduced with pre-miR-101 transfection and increased with anti-miR-101 transfection **(A)**. Mir-101 inhibition similarly increased the relative mRNA expression (normalized to β-actin) of EZH2α and EZH2β **(B)**. All data are presented as mean ± SEM. **P*<0.05 and ***P*<0.01 and *vs.* GDM-Scr. The number of donors used to prepare the tested HUVECs is reported in each panel.

In addition, pre-miR-101 decreased EZH2 protein (Figure 4.12 A) and H3K27m3 expression compared to the scramble control (Figure 4.12 B). Finally, anti-miR-101 increased EZH2 in GDM-HUVECs (Figure 4.12 A), but it did not change the overall H3K27m3 protein expression, as shown by Western blotting analysis (Figure 4.12 B).

From these experiments we concluded that miR-101 targets EZH2 in GDM-HUVECs and downregulates its expression.

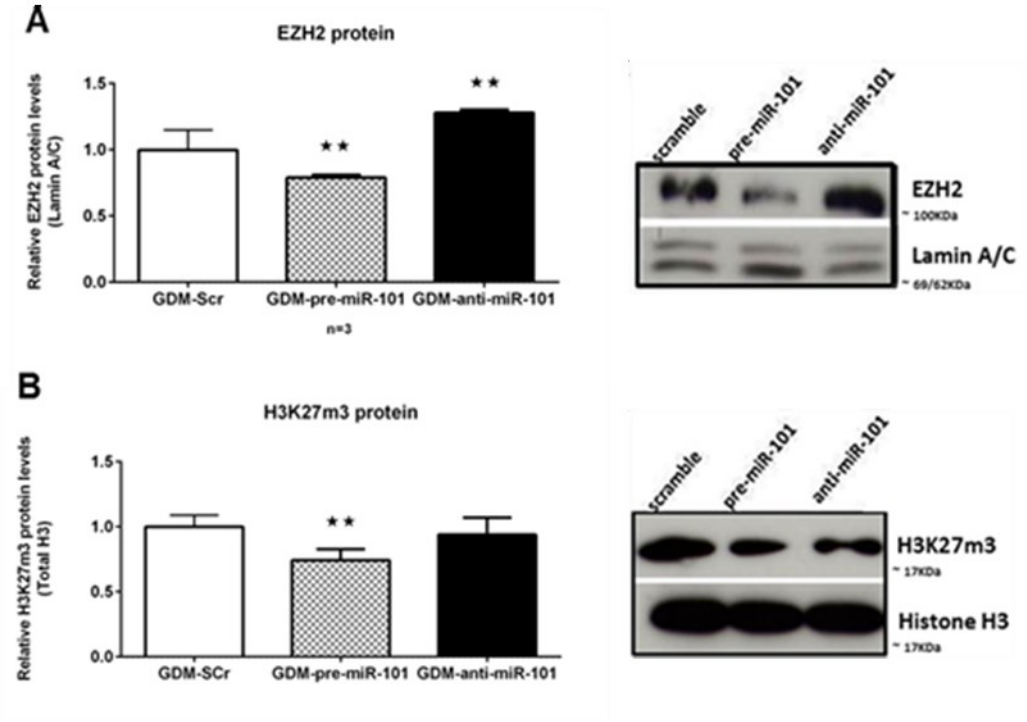


Figure 4.12: MiR-101 regulates EZH2 and H3K27m3 protein levels in GDM HUVECs
The protein expression of EZH2 (normalized to laminin A/C) and H3K27me3 (normalized to H3) was negatively altered in GDM-HUVECs transfected with pre-miR-101, whereas anti-miR-101 increased EZH2 **(A)**, but not H3K27m3 protein **(B)**. All data are expressed as mean ± SEM. **P*<0.05 and ***P*<0.01 *vs.* GDM-Scr group. The number of donors used to prepare the tested HUVECs is reported in each panel.

4.7 GDM reduces EZH2 and H3K27m3 occupancy at the miR-101 locus transcriptional regulatory region.

Similar to protein coding genes, miRNAs are also susceptible to epigenetic modulation suggesting the existence of a regulatory circuit between epigenetic and miRNAs [95] In this context it has been demonstrated that EZH2 regulates miR-101 in ovarian cancer cells [115]

To understand whether EZH2 regulates miR-101 in GDM-HUVECs we looked at EZH2 and H3K27m3 occupancy within the promoter of the miR-101 locus. A scheme of the miR-101 promoter is presented as Figure 4.13.

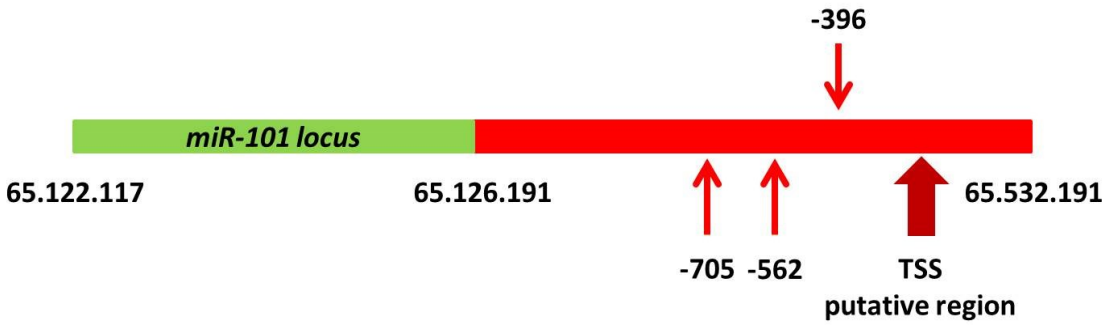


Figure 4.13: Scheme of miR-101 promoter regions
Representation of the transcriptional location of the miR-101-1 gene (Ch1: 65.522.117–65.526.191) derived from the University of California Santa Cruz (UCSC), Genome Browser GRCh37/ hg19. The red arrows show the transcription starting site (TSS) putative region and the regions amplified by the three set of primers used for the chromatin immunoprecipitation (ChIP).

By performing chromatin immunoprecipitation (ChIP) with antibodies targeting EZH2 and H3K27m3, followed by qPCR for different miR-101 promoter regions (Table III, Materials and Methods), we found that EZH2 and H3K27m3 occupy the miR-101 promoter in both healthy HUVECs and GDM-HUVECs (Figure 4.14 A). Moreover, in GDM-HUVECs, we observed decreased EZH2 and H3K27m3 occupancy at a regulatory sequence beginning at −396 bp upstream of the transcription start site (TSS), (Figure 4.14 A).

Taking into consideration current paradigms, it is expected that reduced EZH2 occupancy on the miR-101 promoter results in a higher accessibility of chromatin, thereby increasing miR-101 transcription in GDM-HUVECs. Indeed by performing

qPCR on GDM-HUVECs transfected with small interfering RNA for EZH2 (siEZH2), we found increased miR-101 expression (≈ 3.5 fold increase ± 0,564, *P*<0.05) after EZH2 silencing compared to a siRNA scramble sequence (siRNA-Scr) (Figure 4.14 B).

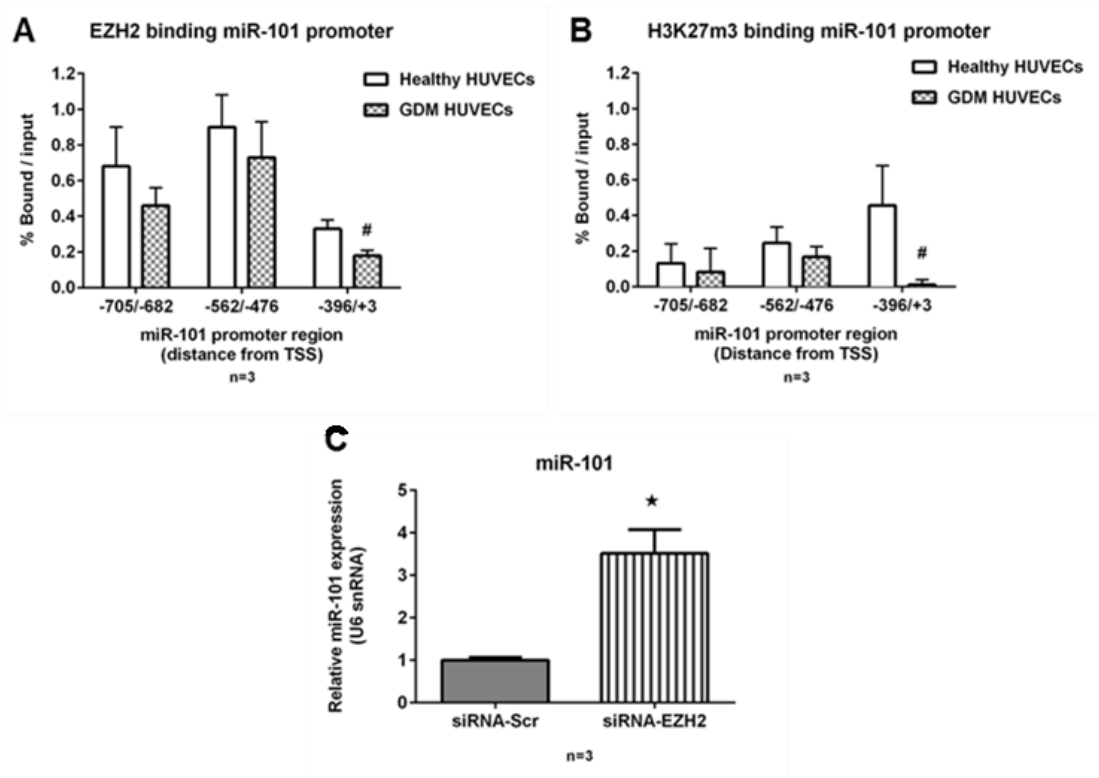


Figure 4.14: EZH2 regulates the promoter methylation status of miR-101
Chromatin immunoprecipitation (ChIP) followed by qPCR showed that EZH2 occupancy on the transcriptional regulatory region (−396/+3 bp from the transcription start site [TSS]) of the miR-101 promoter was reduced in GDM-HUVECs compared to Healthy-HUVECs **(A)**, and consistently also H3K27m3 binding to this promoter region was decreased in GDM-HUVECs **(B)**. IgG was used as a negative control. Data were calculated as % bound/input. Relative miR-101 expression level (normalized to snRNAU6) increased in GDM-HUVECs transfected with small interfering RNA for EZH2 (siRNA-EZH2) compared with cells transfected with a siRNA scrambled sequence (siRNA-Scr) **(C)**. All data are expressed as mean ± SEM. #*P*<0.05 *vs.* Healthy-HUVECs; **P*<0.05 *vs.* siRNA-Scr. The number of donors used to prepare the tested HUVECs is reported in each panel.

4.8 EZH2β inhibits miR-101 transcription in HUVECs

To complement these studies, we performed luciferase reporter assays on healthy HUVECs overexpressing either EZH2α or EZH2β. Figure 4.15 shows that Ad-mediated EZH2β overexpression inhibits the transcriptional activity of the miR-101 promoter in

comparison with Ad.Null and EZH2α. EZH2α did not exert any significant effect on miR-101 promoter transcriptional activity. Taken together, these results suggested that in HUVECs miR-101 transcription is regulated by EZH2, specifically by the EZH2β isoform.

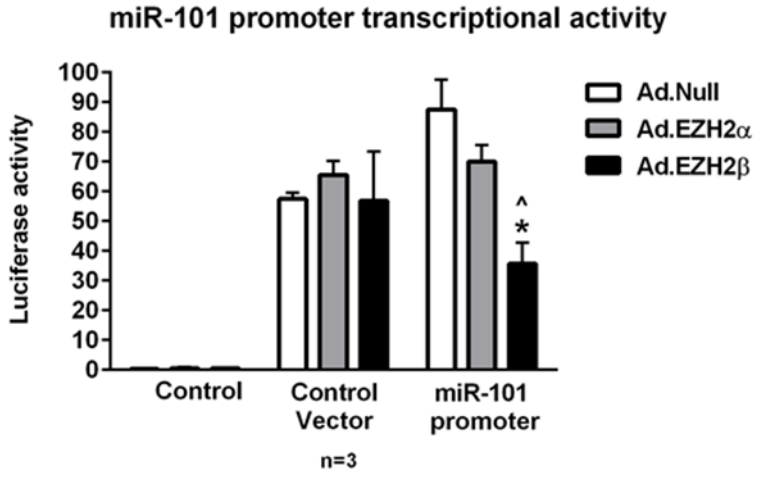


Figure 4.15: MiR-101 transcription in HUVECs is regulated by EZH2β
Transcription reporter assay performed in healthy HUVECs showed a significant decrease of miR-101 promoter activity after Ad-mediated EZH2β but not after EZH2α overexpression compared to Ad.Null. **P*<0.05 *vs.* Ad.Null and $^{\wedge}$*P*<0.05 *vs.* Ad.EZH2α. The number of donors used to prepare the tested HUVECs is reported in each panel.

4.9 *In vitro* exposure of healthy HUVECs to high concentrations of glucose lowers EZH2 binding to the miR-101 promoter and increases miR-101 expression

Next, we wanted to investigate whether exposure of normal HUVECs to high concentrations of glucose (HG) *in vitro* may recapitulate the molecular changes observed in HUVECs from GDM pregnancies.

To this end, healthy HUVECs were exposed to high (25 mM) or normal glucose concentrations (5 mM) for 48 hours, using L-glucose as an osmotic control (20 mM). ChIP was used to measure EZH2 binding to the abovementioned miR-101 promoter region beginning at around −396 bp upstream of the TSS. Indeed, similar to GDM, we found that *in vitro* cell exposure to HG reduced the presence of EZH2 at this miR-101

promoter regulatory region (Figure 4.16 A). Moreover, congruent with the results from ChIP assays, HG increased miR-101 levels in healthy HUVECs (Figure 4.16 B).

Taken together, our data suggest that EZH2 and miR-101 are reciprocally regulated in HUVECs and that an imbalance of this equilibrium in response to either *in vivo* GDM or *in vitro* exposure to HG might result in a lower EZH2 occupancy of the miR-101 locus, thus leading to increased miR-101 transcription and further phenotypic alterations of ECs.

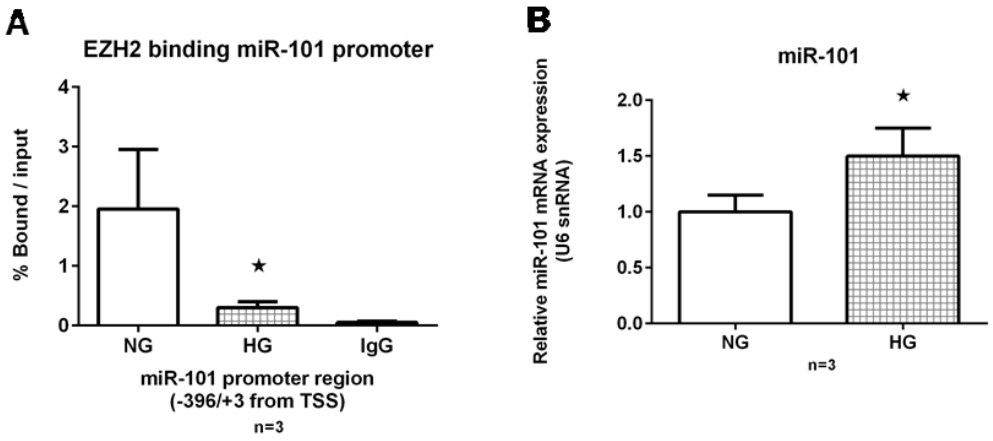


Figure 4.16: Exposure to high glucose (HG) reduces EZH2 occupancy at the miR-101 promoter in HUVECs
Healthy HUVECs were exposed to normal D-glucose (NG; 5 mmol/L) or high D-glucose concentrations (HG, 25 mmol/L), with 20 mmol/L L-glucose as an osmotic control, for 48 hours. HG was intended to mimic diabetic hyperglycemia. ChIP analysis followed by qPCR revealed a lower EZH2 occupancy at the miR-101 locus regulatory region (−396/+3 bp from the TSS) under HG. IgG was used as a negative control. Data were calculated as % bound/input. **(A)**. MiR-101 expression was increased in HG compared with NG with osmotic control **(B)**. All data were expressed as mean ± SEM, **P*<0.05 *vs*. NG.

4.10 Effect of EZH2 overexpression on phenotypic alterations in GDM-HUVECs

To see whether restoring EZH2 levels in GDM-HUVECs could rescue the cell survival, proliferation and angiogenic capabilities, we transduced GDM-HUVECs with Ad.EZH2α or Ad.EZH2β using an empty vector as control (Ad Null). Ad.EZH2β decreased the relative apoptotic activity (Figure 4.17 A) but did not rescue impaired proliferation (Figure 4.17 B). Moreover Ad.EZH2β increased the migratory capacity of GDM-HUVECs (Figure 4.17 C) but did not have any effect on tube formation (Figure

4.17 D). Ad.EZH2-α did not alter the behavior of GDM-HUVECs (Figures 4.17A-4.17D). Taken together, these data suggest that a deficit in EZH2β contributes to some of the functional defects induced by GDM in fetal endothelial cells.

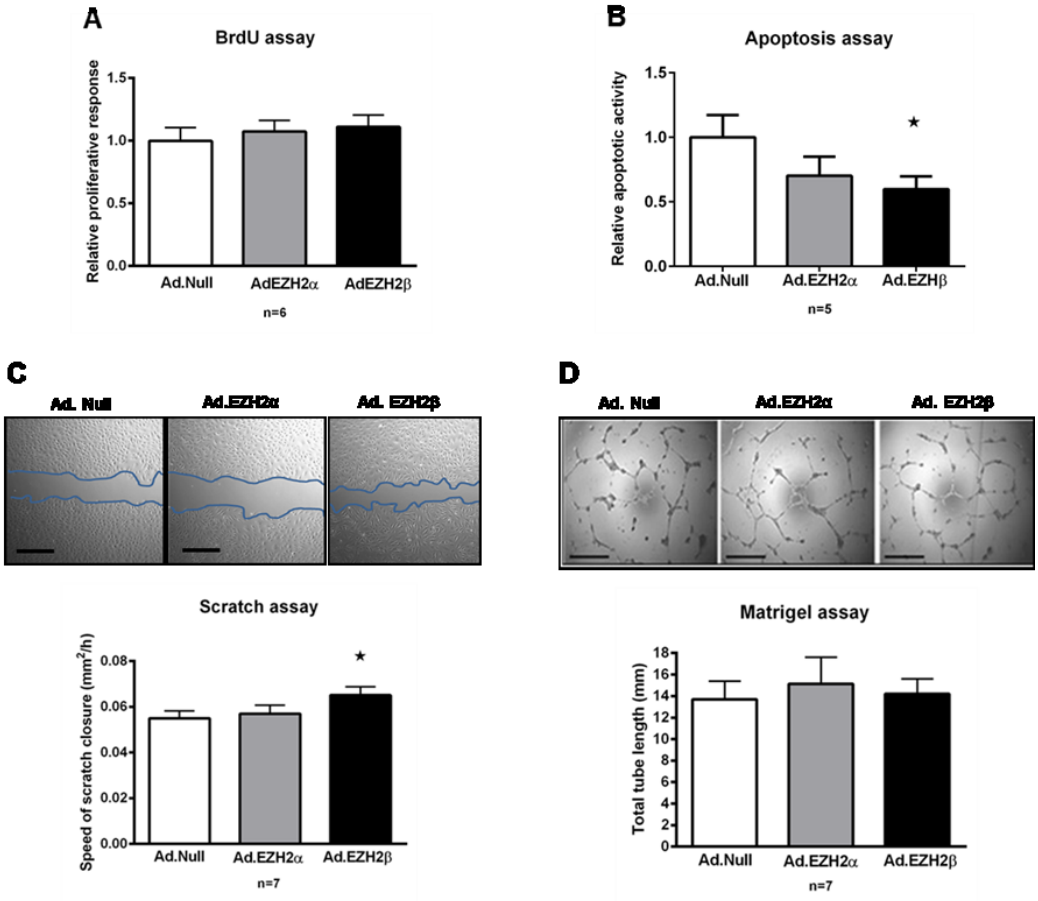


Figure 4.17 Effect of Ad.-mediated EZH2 overexpression on functional capacities of GDM-HUVECs

GDM-HUVECs were infected with adenovirus carrying EZH2α, EZH2β, or an empty vector (Ad.Null). Ad.EZH2β rescued GDM-HUVEC survival **(A)** and showed no effect on cell proliferation **(B)**. Moreover, Ad.EZH2β improved the migration capacity of GDM-HUVECs **(C)**, whereas it exerted no effect on tube formation (presented here as tube length in mm) **(D)**. In all tests, Ad.EZH2α produced a similar effect to Ad.Null. (Scale bars 0.5 mm). Data are presented as mean ± SEM. **P*<0.05 *vs.* Ad.Null. The number of donors used to prepare the tested HUVECs is reported in each panel.

Chapter V – Discussion and Conclusions

Gestational diabetes mellitus (GDM) is a common medical complication in pregnancy and is associated with adverse long-term outcomes for the offspring. GDM leads to fetal hyperglycemia and endothelial dysfunction in the fetal circulation where it might be responsible for the increased incidence of type 2 diabetes (T2D) and cardiovascular disease (CVD) observed later in life [2–4]. Clinical trials and epidemiological studies in patients with either T1D or T2D have demonstrated that exposure to prolonged hyperglycemia leaves a long-lasting impression on vascular cells leading to the development of vascular complications which persist even after glycemic control is achieved. However, the same studies also suggested that a good glycemic control can delay the onset of vascular complications in diabetic subjects [5].

Accumulating evidence suggests a key role for epigenetic mechanisms such as DNA methylation, histone post-translational modifications, and non-coding RNAs in the complex interplay between genes and the environment. Factors associated with the pathology of diabetic complications, including hyperglycemia, oxidative stress and inflammatory factors might lead to dysregulation of these epigenetic mechanisms and alter the expression of genes involved in endothelial cell homeostasis, without changes in the underlying DNA sequence. Furthermore, long-term persistence of these alterations may be a key mechanism underlying the phenomenon of "metabolic memory" and progression of endothelial dysfunction despite the achievement of glycemic control. Current strategies to prevent diabetes and its vascular complications have not been fully efficacious [143], thus a study of the epigenetic mechanisms occurring during fetal development in the diabetic environment would represent an early strategy to prevent T2D and CVD in adulthood.

In this study we have provided a novel underlying mechanism involving miR-101 and Enhancer of Zeste Homologue 2 (EZH2), in GDM-elicited fetal endothelial dysfunction. The first goal was to characterize the effect of GDM on fetal endothelial cell (EC) functionality. To this end we have isolated human umbilical vein endothelial cells (HUVECs) from the umbilical cords of GDM mothers. These cells are an expedient *in vitro* model for the study of the molecular consequences of long-term exposure to chronic hyperglycemia. A few studies have shown some biochemical alterations such as impaired NO bioavailability [140] as well as increased adhesion molecule protein levels [67] in HUVECs isolated from GDM-mothers. Here, we have reported that GDM-HUVECs present an increased rate of apoptosis and a decreased proliferation compared to HUVECs isolated from healthy-pregnancies. Moreover we have found a decrease in migration and angiogenic capabilities, measured by means of

scratch assays and tube formation on Matrigel respectively. These data have provided a functional characterization of GDM-HUVECs contributing to extend the knowledge on the effect of the intrauterine environment on fetal endothelium. Moreover, these analyses have been performed after cells were expanded in normal D-glucose concentrations (5mM) for 5 to 6 passages, suggesting that the cells were still affected by the chronic hyperglycemia sensed *in utero*, which is consistent with the existence of a metabolic memory.

The second objective of this study was to investigate on the role of epigenetic factors and miRNA in the functional alterations observed in diabetic ECs. A previous study has shown that miR-101 regulates endothelial function and angiogenesis by inhibiting EZH2 transcription in ECs under physiological glucose conditions (Smits et al. 2011). Similarly, our data have demonstrated that GDM is associated with an increase of miR-101 expression and a reduction of its target EZH2, mainly of the EZH2β isoform. EZH2 is essential for the epigenetic maintenance of the trimethylation of lysine 27 on histone H3 (H3K27me3) [112] and its decrease would lead to a reduction of the H3K27me3 mark, as we have found in GDM-HUVECs, and subsequently to a diminution of EZH2-mediated gene silencing. Accordingly, a recent study has identified 946 genes upregulated by >2-fold due to EZH2 knockdown, in line with its repressive function. Importantly, many of these genes are implicated in endothelial cell dysfunction and cardiovascular disease [116].

In this study we have found a novel underlying mechanism involving miR-101 and EZH2 in GDM endothelial dysfunction. We have identified that in HUVECs, EZH2 is both a target of, and a transcriptional repressor for, miR-101. By performing chromatin immunoprecipitation (ChIP) we have shown that increased miR-101 expression, in both GDM-HUVECs and HUVECs exposed to high concentrations of glucose *in vitro* (25mM), is associated with reduced EZH2 binding at transcriptional regulatory regions of the miR-101 gene promoter and reduced H3K27me3 (within 0.5 kb of transcription starting site). The reduced H3K27me3 mark results in higher chromatin accessibility to transcription factors and consequently to an increase in miR-101 transcription. Consistently, we have also shown that EZH2 knockdown increased miR-101 expression in HUVECs. This result is consistent with the knowledge that miRNAs and their target genes are often linked in a regulatory feedback loop, which maintains their homeostatic expressional balance [144]. Additionally, we have found that among the two recently identified EZH2 isoforms [9], EZH2β is the only one which is both a target of GDM and a mediator of some of the GDM-HUVECs' endothelial dysfunction.

Our data also suggest that some defects of GDM are mediated by miR-101 independently of EZH2β. In fact, although miR-101 inhibition rescues most of the studied cell functions in GDM-HUVECs, Ad-mediated EZH2β only improved cell survival and migration. This can be explained with the knowledge that miR-101 acts post-transcriptionally on multiple target genes, including EZH2 and vascular endothelial growth factor A [145]. A possible limitation of our study is that we have not identified all the miR-101 target genes involved with the GDM-induced vascular defects. Moreover, because EZH2 regulates the transcription of different genes, the rescue effect of EZH2β can be mediated by the inhibition of a number of damaging genes.

Taken together, our data suggest that EZH2 and miR-101 are reciprocally regulated in HUVECs; EZH2 is both a target of and a transcriptional repressor for miR-101. In GDM this equilibrium is compromised resulting in a lower EZH2β occupancy of the miR-101 promoter, thus leading to increased miR-101 transcription and further phenotypic alterations of ECs. This altered miR-101/EZH2 equilibrium could continue to influence vascular gene expression and function well after birth thus contributing to the cardiovascular complications of GDM in the offspring.

Our study is in line with the concept of a "glycemic memory" where *in vivo* or *in vitro* exposure to chronic hyperglycemia leads to persistent changes in vascular cells, through dysregulation of the underlining epigenetic mechanisms.

This findings provide new insights about the epigenetic pathways activated by GDM *in utero*, providing new targets for future therapeutic interventions. MiRNA-based therapeutics is still in the early stages; however, inhibition of some miRNAs has been promising for the future treatment of vascular diseases [134,135]. With the focus on the observed changes in EZH2 levels, it would appear conceivable to target miR-101 for inhibition in GDM.

In future studies, it would be worth attempting to correlate miR-101 levels in HUVECs with its levels both in the fetal and in the maternal blood at different phases of pregnancy. This could lead to the development of miR-101 as a circulating biomarker of fetal endothelial damage induced by GDM.

Chapter VI – References

1. American Diabetes Association. Standards of medical care in diabetes-2010. *Diabetes Care* **33,** 11–61 (2010).

2. Dabelea, D. & Pettitt, D. J. Intrauterine diabetic environment confers risks for type 2 diabetes mellitus and obesity in the offspring, in addition to genetic susceptibility. *J Pediatr Endocrinol Metab* **14,** 1085–1091 (2001).

3. Pettitt, D. J. *et al.* Association between maternal diabetes in utero and age at offspring's diagnosis of type 2 diabetes. *Diabetes Care* **31,** 2126–30 (2008).

4. Franks, P. W. *et al.* Gestational glucose tolerance and risk of type 2 diabetes in young Pima Indian offspring. *Diabetes* **55,** 460–5 (2006).

5. Nathan, D. M. *et al.* Intensive diabetes treatment and cardiovascular disease in patients with type 1 diabetes. *N. Engl. J. Med.* **353,** 2643–53 (2005).

6. Bird, A. Perceptions of epigenetics. *Nature* **447,** 396–8 (2007).

7. Zhang, X. & Ho, S.-M. Epigenetics meets endocrinology. *J. Mol. Endocrinol.* **46,** R11–32 (2011).

8. Cooper, M. E. & El-Osta, A. Epigenetics: Mechanisms and implications for diabetic complications. *Circ. Res.* **107,** 1403–1413 (2010).

9. Grzenda, A. *et al.* Functional characterization of EZH2β reveals the increased complexity of EZH2 isoforms involved in the regulation of mammalian gene expression. *Epigenetics Chromatin* **6,** 3 (2013).

10. Sander, S. *et al.* MYC stimulates EZH2 expression by repression of its negative regulator miR-26a. *Blood* **112,** 4202–4212 (2008).

11. Juan, A. H., Kumar, R. M., Marx, J. G., Young, R. A. & Sartorelli, V. Mir-214-Dependent Regulation of the Polycomb Protein Ezh2 in Skeletal Muscle and Embryonic Stem Cells. *Mol. Cell* **36,** 61–74 (2009).

12. Smits, M. *et al.* Down-regulation of miR-101 in endothelial cells promotes blood vessel formation through reduced repression of EZH2. *PLoS One* **6,** (2011).

13. The Expert Committee on the Diagnosis and Classification of Diabetes. Report of the Expert Committee on the diagnosis and classification of diabetes mellitus. *Diabetes Care* **26,** S5–20 (2003).

14. Lawrence, J. M., Contreras, R., Chen, W. & Sacks, D. a. Trends in the Prevalence of Preexisting Diabetes and Gestational Diabetes Mellitus Among a Racially / Ethnically Diverse Population of Pregnant Women ,. *Diabetes Care* **31,** 899–904 (2008).

15. American Diabetes Association. Diagnosis and classification of diabetes mellitus. *Diabetes Care* **37 Suppl 1,** S81–90 (2014).

16. Galtier, F. Definition, epidemiology, risk factors. *Diabetes Metab.* **36,** 628–651 (2010).

17. Shaw, J. E., Sicree, R. a. & Zimmet, P. Z. Global estimates of the prevalence of diabetes for 2010 and 2030. *Diabetes Res. Clin. Pract.* **87,** 4–14 (2010).

18. Barbour, L. a. *et al.* Cellular mechanisms for insulin resistance in normal pregnancy and gestational diabetes. *Diabetes Care* **30,** 112–119 (2007).

19. Robinson, R. E. Clinical aspects of diabetes in pregnancy. *Postgrad. Med. J.* **55,** 358–61 (1979).

20. Poulakos, P. *et al.* Comments on gestational diabetes mellitus: from pathophysiology to clinical practice. *Hormones (Athens).* (2015). doi:10.14310/horm.2002.1570

21. Crowther, C. a *et al.* Effect of treatment of gestational diabetes mellitus on pregnancy outcomes. *N. Engl. J. Med.* **352,** 2477–86 (2005).

22. Dodd, J. M., Crowther, C. A., Antoniou, G., Baghurst, P. & Robinson, J. S. Screening for gestational diabetes: the effect of varying blood glucose definitions in the prediction of adverse maternal and infant health outcomes. *Aust N Z J Obs. Gynaecol* **47,** 307–312 (2007).

23. Clausen, T. D. *et al.* High prevalence of type 2 diabetes and pre-diabetes in adult offspring of women with gestational diabetes mellitus or type 1 diabetes: the role of intrauterine hyperglycemia. *Diabetes Care* **31,** 340–6 (2008).

24. Ferrara A. & Elhrich S.F. Strategies for diabetes prevention before and after pregnancy in women with GDM. *Current Diabetes Reviews* **7,** 75–83 (2011).

25. Feig, D. S., Zinman, B., Wang, X. & Hux, J. E. Risk of development of diabetes mellitus after diagnosis of gestational diabetes. *CMAJ* **179,** 229–34 (2008).

26. Lee, A. J., Hiscock, R. J., Wein, P., Walker, S. P. & Permezel, M. Gestational diabetes mellitus: Clinical predictors and long-term risk of developing type 2 Diabetes - A retrospective cohort study using survival analysis. *Diabetes Care* **30,** 878–883 (2007).

27. Shah, B. R., Retnakaran, R. & Booth, G. L. Increased risk of cardiovascular disease in young women following gestational diabetes mellitus. *Diabetes Care* **31,** 1668–9 (2008).

28. Freinkel, N. Banting Lecture 1980. Of pregnancy and progeny. *Diabetes* **29,** 1023–1035 (1980).

29. Hales, C. N. & Barker, D. J. P. Type 2 (non-insulin-dependent) diabetes mellitus: the thrifty phenotype hypothesis. *Int. J. Epidemiol.* **42,** 1215–1222 (2013).

30. Kyle, U. G. & Pichard, C. The Dutch Famine of 1944-1945: a pathophysiological model of long-term consequences of wasting disease. *Curr. Opin. Clin. Nutr. Metab. Care* **9,** 388–94 (2006).

31. Roseboom, T., de Rooij, S. & Painter, R. The Dutch famine and its long-term consequences for adult health. *Early Hum. Dev.* **82,** 485–91 (2006).

32. Fernández-Morera, J. L., Rodríguez-Rodero, S., Menéndez-Torre, E. & Fraga, M. F. The possible role of epigenetics in gestational diabetes: cause, consequence, or both. *Obs. Gynecol Int* **2010,** 605163 (2010).

33. Ben-Haroush, a, Yogev, Y. & Hod, M. Epidemiology of gestational diabetes mellitus and its association with Type 2 diabetes. *Diabet. Med.* **21,** 103–113 (2004).

34. Karagiannis, T., Bekiari, E., Manolopoulos, K., Paletas, K. & Tsapas, a. Gestational diabetes mellitus: Why screen and how to diagnose. *Hippokratia* **14,** 151–154 (2010).

35. O'Sullivan, J. B., Mahan, C. M., Charles, D. & Dandrow, R. V. Screening criteria for high risk gestational diabetic patients. *Am. J. Obstet. Gynecol.* **116,** 895–900 (1973).

36. National Diabetes Data Group. Classification and Diagnosis of Diabetes Mellitus and Other Categories of Glucose Intolerance. *Diabetes* **28,** 1039–1057 (1979).

37. Carpenter, M. W. & Coustan, D. R. Criteria for screening tests for gestational diabetes. *American journal of obstetrics and gynecology* **144,** 768–773 (1982).

38. Metzger, B. E. *et al.* Hyperglycemia and adverse pregnancy outcomes. *N. Engl. J. Med.* **358,** 1991–2002 (2008).

39. Coustan, D. R., Lowe, L. P., Metzger, B. E. & Dyer, A. R. The Hyperglycemia and Adverse Pregnancy Outcome (HAPO) study: paving the way for new diagnostic criteria for gestational diabetes mellitus. *Am. J. Obstet. Gynecol.* **202,** 1–6 (2010).

40. The HAPO Study Cooperative Research Group. The Hyperglycemia and Adverse Pregnancy Outcome (HAPO) Study. *Int. J. Gynaecol. Obstet.* **78,** 69–77 (2002).

41. Claesson, R., Ekelund, M. & Berntorp, K. The potential impact of new diagnostic criteria on the frequency of gestational diabetes mellitus in Sweden. *Acta Obs. Gynecol Scand* **92,** 1223–1226 (2013).

42. Blumer, I. *et al.* Diabetes and pregnancy: an endocrine society clinical practice guideline. *J. Clin. Endocrinol. Metab.* **98,** 4227–49 (2013).

43. Landon, M. B. *et al.* A multicenter, randomized trial of treatment for mild gestational diabetes. *N. Engl. J. Med.* **361,** 1339–1348 (2009).

44. Lapolla, A., Dalfrà, M. G. & Fedele, D. Management of gestational diabetes mellitus. *Diabetes. Metab. Syndr. Obes.* **2,** 73–82 (2009).

45. Reader, D., Splett, P. & Gunderson, E. P. Impact of Gestational Diabetes Mellitus Nutrition Practice Guidelines Implemented by Registered Dietitians on Pregnancy Outcomes. *J. Am. Diet. Assoc.* **106,** 1426–1433 (2006).

46. Homko, C. J. & Reece, E. A. Insulins and oral hypoglycemic agents in pregnancy. *J. Matern. Fetal. Neonatal Med.* **19,** 679–86 (2006).

47. Rowan, J. A. . *et al.* Metformin versus Insulin for the Treatment of Gestational Diabetes. *N. Engl. J. Med.* **358,** 2003–15 (2008).

48. Langer, O., Conway, D. L., Berkus, M. D., Xenakis, E. M. & Gonzales, O. A comparison of glyburide and insulin in women with gestational diabetes mellitus. *Engl. J.* **343,** 1134–1138 (2000).

49. Dhulkotia, J. S., Ola, B., Fraser, R. & Farrell, T. Oral hypoglycemic agents vs insulin in management of gestational diabetes: A systematic review and metaanalysis. *Am. J. Obstet. Gynecol.* **203,** 457–459 (2010).

50. Kaiser, N. *et al.* Differential regulation of glucose transport and transporters by glucose in vascular endothelial and smooth muscle cells. *Diabetes* **42,** 80–89 (1993).

51. Heilig, C. W. *et al.* Overexpression of glucose transporters in rat mesangial cells cultured in a normal glucose milieu mimics the diabetic phenotype. *J. Clin. Invest.* **96,** 1802–1814 (1995).

52. Baynes, J. W. Role of oxidative stress in development of complications in diabetes. *Diabetes* **40,** 405–412 (1991).

53. Brownlee, M. Biochemistry and molecular cell biology of diabetic complications. *Nature* **414,** 813–820 (2001).

54. Clempus, R. E. & Griendling, K. K. Reactive oxygen species signaling in vascular smooth muscle cells. *Cardiovasc. Res.* **71,** 216–225 (2006).

55. Brownlee, M. Biochemistry and molecular cell biology of diabetic complications. *Nature* **414,** 813–820 (2001).

56. Ishii, H., Koya, D. & King, G. L. Protein kinase C activation and its role in the development of vascular complications in diabetes mellitus. *J. Mol. Med. (Berl).* **76,** 21–31 (1998).

57. Kim, W. *et al.* Receptor for advanced glycation end products and its ligands: a journey from the complications of diabetes to its pathogenesis. *Ann. N. Y. Acad. Sci.* **1043,** 553–61 (2005).

58. Brownlee, M. The Pathobiology of Diabetic Complications A Unifying Mechanism. *Diabetes* **54,** 1615–1625 (2005).

59. Brosius, F. C., Khoury, C. C., Buller, C. L. & Chen, S. Abnormalities in signaling pathways in diabetic nephropathy. *Expert Rev. Endocrinol. Metab.* **5,** 51–64 (2010).

60. Kanwar, Y. S. *et al.* Diabetic nephropathy: mechanisms of renal disease progression. *Exp. Biol. Med. (Maywood).* **233,** 4–11 (2008).

61. Devaraj, S. *et al.* Increased monocytic activity and biomarkers of inflammation in patients with type 1 diabetes. *Diabetes* **55,** 774–9 (2006).

62. Shanmugam, N., Gaw Gonzalo, I. T. & Natarajan, R. Molecular mechanisms of high glucose-induced cyclooxygenase-2 expression in monocytes. *Diabetes* **53,** 795–802 (2004).

63. Mooradian, A. Dyslipidemia in type 2 diabetes mellitus. *Nat. Clin. Pract. Endocrinol. Metab.* **5,** 150–9 (2009).

64. King, G. L. The Role of Inflammatory Cytokines in Diabetes and Its Complications. *J. Periodontol.* **79,** 1527–1534 (2008).

65. Baumgartner-Parzer, S. M. *et al.* High-glucose-triggered apoptosis in cultured endothelial cells. *Diabetes* **44,** 1323–1327 (1995).

66. Westermeier, F. *et al.* Insulin restores gestational diabetes mellitus-reduced adenosine transport involving differential expression of insulin receptor isoforms in human umbilical vein endothelium. *Diabetes* **60,** 1677–1687 (2011).

67. Di Fulvio, P. *et al.* Features of endothelial dysfunction in umbilical cord vessels of women with gestational diabetes. *Nutr. Metab. Cardiovasc. Dis.* **24,** 1337–1345 (2014).

68. Nold, J. L. & Georgieff, M. K. Infants of diabetic mothers. *Pediatr. Clin. North Am.* **51,** 619–37, viii (2004).

69. Catalano, P. M. & Hauguel-De Mouzon, S. Is it time to revisit the Pedersen hypothesis in the face of the obesity epidemic? *Am. J. Obstet. Gynecol.* **204,** 479–87 (2011).

70. Madamanchi, N. R. & Runge, M. S. Mitochondrial dysfunction in atherosclerosis. *Circ. Res.* **100,** 460–73 (2007).

71. The Diabetes Control and Complications Trial Research Group. The effect of intensive treatment of diabetes on the development and progression of long-term complications in insulin-dependent diabetes mellitus. *N. Engl. J. Med.* **329,** 977–86 (1993).

72. Colagiuri, S., Cull, C. A. & Holman, R. R. Are lower fasting plasma glucose levels at diagnosis of type 2 diabetes associated with improved outcomes?: U.K. prospective diabetes study 61. *Diabetes Care* **25,** 1410–7 (2002).

73. Kowluru, R. a. Effect of reinstitution of good glycemic control on retinal oxidative stress and nitrative stress in diabetic rats. *Diabetes* **52,** 818–823 (2003).

74. Gaede, P., Lund-Andersen, H., Parving, H.-H. & Pedersen, O. Effect of a multifactorial intervention on mortality in type 2 diabetes. *N. Engl. J. Med.* **358,** 580–591 (2008).

75. Engerman, R. L. & Kern, T. S. Progression of incipient diabetic retinopathy during good glycemic control. *Diabetes* **36,** 808–12 (1987).

76. Hammes, H. P. *et al.* Islet transplantation inhibits diabetic retinopathy in the sucrose-fed diabetic Cohen rat. *Invest Ophthalmol Vis Sci* **34,** 2092–2096 (1993).

77. Chan, P. S., Kanwar, M. & Kowluru, R. a. Resistance of retinal inflammatory mediators to suppress after reinstitution of good glycemic control: novel mechanism for metabolic memory. *J. Diabetes Complications* **24,** 55–63 (2010).

78. Roy, S., Sala, R., Cagliero, E. & Lorenzi, M. Overexpression of fibronectin induced by diabetes or high glucose: phenomenon with a memory. *Proc. Natl. Acad. Sci. U. S. A.* **87,** 404–408 (1990).

79. Brasacchio, D. *et al.* Hyperglycemia Induces a Dynamic Cooperativity of Histone Methylase and Demethylase Enzymes Associated With Gene-Activating Epigenetic Marks That Coexist on the Lysine Tail. *Diabetes* **58,** 1229–1236 (2009).

80. El-Osta, A. *et al.* Transient high glucose causes persistent epigenetic changes and altered gene expression during subsequent normoglycemia. *J. Exp. Med.* **205,** 2409–2417 (2008).

81. Ihnat, M. a. *et al.* Reactive oxygen species mediate a cellular 'memory' of high glucose stress signalling. *Diabetologia* **50,** 1523–1531 (2007).

82. Kouzarides, T. Chromatin modifications and their function. *Cell* **128,** 693–705 (2007).

83. Zhang, Y. & Reinberg, D. Transcription regulation by histone methylation: Interplay between different covalent modifications of the core histone tails. *Genes Dev.* **15,** 2343–2360 (2001).

84. Martin, C. & Zhang, Y. The diverse functions of histone lysine methylation. *Nat. Rev. Mol. Cell Biol.* **6,** 838–849 (2005).

85. Shi, Y. *et al.* Histone demethylation mediated by the nuclear amine oxidase homolog LSD1. *Cell* **119,** 941–953 (2004).

86. Metzger, E. *et al.* LSD1 demethylates repressive histone marks to promote androgen-receptor-dependent transcription. *Nature* **437,** 436–439 (2005).

87. Whetstine, J. R. *et al.* Reversal of Histone Lysine Trimethylation by the JMJD2 Family of Histone Demethylases. *Cell* **125,** 467–481 (2006).

88. Tateishi, K., Okada, Y., Kallin, E. M. & Zhang, Y. Role of Jhdm2a in regulating metabolic gene expression and obesity resistance. *Nature* **458,** 757–61 (2009).

89. Sarraf, S. a. & Stancheva, I. Methyl-CpG binding protein MBD1 couples histone H3 methylation at lysine 9 by SETDB1 to DNA replication and chromatin assembly. *Mol. Cell* **15,** 595–605 (2004).

90. Francis, N. J., Follmer, N. E., Simon, M. D., Aghia, G. & Butler, J. D. Polycomb proteins remain bound to chromatin and DNA during DNA replication in vitro. *Cell* **137,** 110–22 (2009).

91. Hansen, K. H. *et al.* A model for transmission of the H3K27me3 epigenetic mark. *Nat. Cell Biol.* **10,** 1291–300 (2008).

92. Chen, H. *et al.* Polycomb protein Ezh2 regulates pancreatic β-cell Ink4a / Arf expression and regeneration in streptozotocin-induced diabetes mellitus. *Insulin* 975–985 (2009). doi:10.1101/gad.1742509.regenerative

93. Bartel, D. P. MicroRNAs: target recognition and regulatory functions. *Cell* **136,** 215–33 (2009).

94. Yang, J.-S. & Lai, E. C. Alternative miRNA biogenesis pathways and the interpretation of core miRNA pathway mutants. *Mol. Cell* **43,** 892–903 (2011).

95. Barski, A. *et al.* Chromatin poises miRNA- and protein-coding genes for expression. *Genome Res.* **19,** 1742–51 (2009).

96. Croce, C. M. & Cain, G. A. miRNAs, Cancer, and Stem Cell Division. *Cell* **122,** 4–6 (2005).

97. Heneghan, H. M., Miller, N. & Kerin, M. J. Role of microRNAs in obesity and the metabolic syndrome. *Obes. Rev.* **11,** 354–61 (2010).

98. Poy, M. N. *et al.* A pancreatic islet-specific microRNA regulates insulin secretion. *Nature* **432,** 226–230 (2004).

99. Kuehbacher, A., Urbich, C., Zeiher, A. M. & Dimmeler, S. Role of Dicer and Drosha for endothelial microRNA expression and angiogenesis. *Circ. Res.* **101,** 59–68 (2007).

100. Suárez, Y. *et al.* Dicer-dependent endothelial microRNAs are necessary for postnatal angiogenesis. *Proc. Natl. Acad. Sci. U. S. A.* **105,** 14082–14087 (2008).

101. Poliseno, L. *et al.* MicroRNAs modulate the angiogenic properties of HUVECs. *Blood* **108,** 3068–3071 (2006).

102. Suárez, Y., Fernández-Hernando, C., Pober, J. S. & Sessa, W. C. Dicer dependent microRNAs regulate gene expression and functions in human endothelial cells. *Circ. Res.* **100,** 1164–1173 (2007).

103. Ren, X.-P. *et al.* MicroRNA-320 is involved in the regulation of cardiac ischemia/reperfusion injury by targeting heat-shock protein 20. *Circulation* **119,** 2357–66 (2009).

104. Caporali, A. *et al.* Deregulation of microRNA-503 contributes to diabetes mellitus-induced impairment of endothelial function and reparative angiogenesis after limb ischemia. *Circulation* **123,** 282–291 (2011).

105. Long, J., Wang, Y., Wang, W., Chang, B. H. J. & Danesh, F. R. MicroRNA-29c is a signature MicroRNA under high glucose conditions that targets sprouty homolog 1, and its in vivo knockdown prevents progression of diabetic nephropathy. *J. Biol. Chem.* **286,** 11837–11848 (2011).

106. Li, Y. *et al.* MicroRNA-221 regulates high glucose-induced endothelial dysfunction. *Biochem Biophys Res Commun* **381,** 81–83 (2009).

107. Friedman, J. M. *et al.* The putative tumor suppressor microRNA-101 modulates the cancer epigenome by repressing the polycomb group protein EZH2. *Cancer Res.* **69,** 2623–2629 (2009).

108. Varambally, S. *et al.* Genomic loss of microRNA-101 leads to overexpression of histone methyltransferase EZH2 in cancer. *Science* **322,** 1695–1699 (2008).

109. Smits, M. *et al.* miR-101 is down-regulated in glioblastoma resulting in EZH2-induced proliferation, migration, and angiogenesis. *Oncotarget* **1,** 710–720 (2010).

110. Sparmann, A. & van Lohuizen, M. Polycomb silencers control cell fate, development and cancer. *Nat. Rev. Cancer* **6,** 846–856 (2006).

111. Margueron, R. *et al.* Ezh1 and Ezh2 maintain repressive chromatin through different mechanisms. *Mol. Cell* **32,** 503–18 (2008).

112. Cao, R. *et al.* Role of histone H3 lysine 27 methylation in Polycomb-group silencing. *Science* **298,** 1039–1043 (2002).

113. Margueron, R. & Reinberg, D. The Polycomb complex PRC2 and its mark in life. *Nature* **469,** 343–9 (2011).

114. Lu, C. *et al.* Gene alterations identified by expression profiling in tumor-associated endothelial cells from invasive ovarian carcinoma. *Cancer Res.* **67,** 1757–68 (2007).

115. Kottakis, F. *et al.* FGF-2 Regulates Cell Proliferation, Migration, and Angiogenesis through an NDY1/KDM2B-miR-101-EZH2 Pathway. *Mol. Cell* **43,** 285–298 (2011).

116. Dreger, H. *et al.* Epigenetic regulation of cell adhesion and communication by enhancer of zeste homolog 2 in human endothelial cells. *Hypertension* **60,** 1176–1183 (2012).

117. Mitić, T. *et al.* EZH2 Modulates Angiogenesis In Vitro and in a Mouse Model of Limb Ischemia. *Mol. Ther.* **23,** 32–42 (2014).

118. Benetatos, L., Voulgaris, E., Vartholomatos, G. & Hatzimichael, E. Non-coding RNAs and EZH2 interactions in cancer: Long and short tales from the transcriptome. *Int. J. Cancer* **133,** 267–274 (2013).

119. Vella, S. *et al.* MicroRNA-101 is repressed by EZH2 and its restoration inhibits tumorigenic features in embryonal rhabdomyosarcoma. *Clin. Epigenetics* **7,** 82 (2015).

120. Arroyo, J. D. *et al.* Argonaute2 complexes carry a population of circulating microRNAs independent of vesicles in human plasma. *Proc. Natl. Acad. Sci. U. S. A.* **108,** 5003–8 (2011).

121. Vickers, K. C., Palmisano, B. T., Shoucri, B. M., Shamburek, R. D. & Remaley, A. T. MicroRNAs are transported in plasma and delivered to recipient cells by high-density lipoproteins. *Nat. Cell Biol.* **13,** 423–433 (2011).

122. Valadi, H. *et al.* Exosome-mediated transfer of mRNAs and microRNAs is a novel mechanism of genetic exchange between cells. *Nat. Cell Biol.* **9,** 654–659 (2007).

123. Kroh, E. M., Parkin, R. K., Mitchell, P. S. & Tewari, M. Analysis of circulating microRNA biomarkers in plasma and serum using quantitative reverse transcription-PCR (qRT-PCR). *Methods* **50,** 298–301 (2010).

124. Mitchell, P. S. *et al.* Circulating microRNAs as stable blood-based markers for cancer detection. *Proc. Natl. Acad. Sci. U. S. A.* **105,** 10513–8 (2008).

125. Mraz, M., Malinova, K., Mayer, J. & Pospisilova, S. MicroRNA isolation and stability in stored RNA samples. *Biochem. Biophys. Res. Commun.* **390,** 1–4 (2009).

126. Weber, J. a. *et al.* The microRNA spectrum in 12 body fluids. *Clin. Chem.* **56,** 1733–1741 (2010).

127. Zampetaki, A. *et al.* Plasma microRNA profiling reveals loss of endothelial miR-126 and other microRNAs in type 2 diabetes. *Circ Res* **107,** 810–817 (2010).

128. Guay, C. & Regazzi, R. Circulating microRNAs as novel biomarkers for diabetes mellitus. *Nat. Rev. Endocrinol.* **9,** 513–21 (2013).

129. Bader, A. G., Brown, D. & Winkler, M. The Promise of MicroRNA Replacement Therapy. *Cancer Res.* **70,** 7027–7030 (2010).

130. Seto, A. G. The road toward microRNA therapeutics. *Int. J. Biochem. Cell Biol.* **42,** 1298–305 (2010).

131. Lanford, R. E. *et al.* Therapeutic silencing of microRNA-122 in primates with chronic hepatitis C virus infection. *Science* **327,** 198–201 (2010).

132. Krützfeldt, J. *et al.* Silencing of microRNAs in vivo with 'antagomirs'. *Nature* **438,** 685–689 (2005).

133. Ebert, M. S. & Sharp, P. a. MicroRNA sponges: progress and possibilities. *RNA* **16,** 2043–2050 (2010).

134. Bonauer, A. *et al.* MicroRNA-92a controls angiogenesis and functional recovery of ischemic tissues in mice. *Science* **324,** 1710–3 (2009).

135. Hullinger, T. G. *et al.* Inhibition of miR-15 protects against cardiac ischemic injury. *Circ. Res.* **110,** 71–81 (2012).

136. Pintus, G., Tadolini, B., Posadino, A. M. & Sanna, B. P KC / Raf / MEK / ERK signaling pathway modulates native-LDL- induced E2F-1 gene expression and endothelial cell proliferation. **59,** 934–944 (2003).

137. Zinellu, A. *et al.* S-homocysteinylated LDL apolipoprotein B adversely affects human endothelial cells in vitro. *Atherosclerosis* **206,** 40–46 (2009).

138. Livak, K. J. & Schmittgen, T. D. Analysis of relative gene expression data using real-time quantitative PCR and the 2(-Delta Delta C(T)) Method. *Methods* **25,** 402–408 (2001).

139. Reichman, T. W. *et al.* Selective regulation of gene expression by nuclear factor 110, a member of the NF90 family of double-stranded RNA-binding proteins. *J. Mol. Biol.* **332,** 85–98 (2003).

140. Westermeier, F. *et al.* Equilibrative nucleoside transporters in fetal endothelial dysfunction in diabetes mellitus and hyperglycaemia. *Curr. Vasc. Pharmacol.* **7,** 435–449 (2009).

141. Larrivée, B. & Karsan, A. Isolation and culture of primary endothelial cells. *Methods Mol. Biol.* **290,** 315–29 (2005).

142. Ahmed, G. A. & Golayel, M. K. A. Culture and characterization of Human Umbilical vein endothelial cells. *Egypt. J. Histol.* **29,** 157–164 (2006).

143. Xu, J. & Zou, M.-H. Molecular Insights and Therapeutic Targets for Diabetic Endothelial Dysfunction. *Circulation* **120,** 1266–1286 (2009).

144. Pasquinelli, A. E. MicroRNAs and their targets: recognition, regulation and an emerging reciprocal relationship. *Nat. Rev. Genet.* **13,** 271–282 (2012).

145. Zhang, J., Han, C., Zhu, H., Song, K. & Wu, T. MiR-101 inhibits cholangiocarcinoma angiogenesis through targeting vascular endothelial growth factor (VEGF). *Am. J. Pathol.* **182,** 1629–1639 (2013).

Acknowledgments

I would like to express my special appreciation and thanks to my supervisors Professor Gianfranco Pintus and Professor Costanza Emanueli for all their support and guidance throughout my PhD studies. I am also very grateful for offering me the unique opportunity to complete my PhD studies at the Bristol Heart Institute, which made me develop both my scientific and personal experiences.

I would also like to thanks our collaborators of the Gynaecologic and Obstetric Clinic, Professor Salvatore Dessole and Professor Gianpiero Capobianco for providing us the umbilical cords used for this study.

I am very grateful to Dr. Annamaria Posadino, Dr. Annalisa Cossu and Dr. Roberta Giordo for their precious advices and feedback on my research and for always being so supportive of my work.

I would like to express my sincere gratitude to all my friends the for their constant support and encouragement over the course of my PhD studies.

Most importantly, none of this would have been possible without the encouragement of my family which has been a constant source of love, support and strength.